Supplemental Information: Towards Understanding Prolate 4f Monomers: Numerical Predictions and Experimental Validation of Electronic Properties and Slow Relaxation in a Muffin-shaped Er^{III} Complex

Jan Arneth,[*,†,§] Christian Pachl,[‡,¶,§] Gerlinde Greif,[¶] Birte G. Beier,[†] Peter W. Roesky,[*,¶] Karin Fink,[*,‡] and Rüdiger Klingeler[*,†]

†*Kirchhoff Institute for Physics, Heidelberg University, INF 227, D-69120 Heidelberg, Germany*

‡*Institute of Nanotechnology, Karlsruhe Institute of Technology (KIT), Kaiserstr. 12, 76131 Karlsruhe, Germany*

¶*Institute of Inorganic Chemistry, Karlsruhe Institute of Technology, Kaiserstr. 12, 76131 Karlsruhe, Germany*

§*These authors contributed equally to this work.*

E-mail: jan.arneth@kip.uni-heidelberg.de; roesky@kit.edu; karin.fink@kit.edu; klingeler@kip.uni-heidelberg.de

The Supporting Information contains additional details about the synthesis, structure figures, magnetic susceptibility, HF-EPR and X-ray crystallographic data as well as NMR, IR, mass spectroscopy data. Further information about the numerical results can be found in an additional Supplemental File (ErIII-SI-xyz.zip). The latter includes xyz-files on all model structures used in this paper. The difference between optimized and unoptimized is that in optimized structures, hydrogen positions were optimized on a DFT level as described in the paper. This was done considering all counterions and lattice solvent, so on the "full" structure. Afterwards, the model was truncated to generate the other structures.

1 Synthesis and Crystal Structure

All chemicals were obtained from commercial sources and were used without further purification. 2-(6-((Trimethylsilyl)ethynyl)pyridin-2-yl)-1,10-phenanthroline was prepared according to a literature procedure.[1]

1.1 (4-(6-(1,10-phenanthrolin-2-yl)pyridin-2-yl)-1H-1,2,3-triazol-1-yl)methyl pivalate (PPTMP)

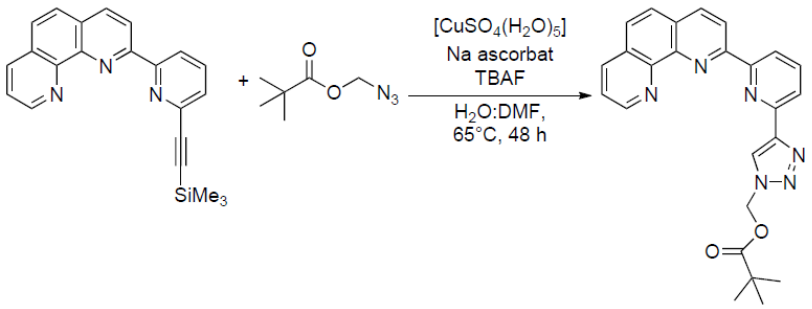

Figure S1: Synthesis scheme of PPTMP.

2-(6-((Trimethylsilyl)ethynyl)pyridin-2-yl)-1,10-phenanthroline (899 mg, 2.54 mmol, 1.00 eq.), azidomethyl pivalate (479 mg, 2,80 mmol, 1.10 eq.), sodium ascorbate (65.5 mg, 0.331 mmol, 0.13 eq.) and copper(II) sulfate pentahydrate (25.4 mg, 0.102 mmol, 0.04 eq.) were dissolved in a DMF:H_2O-mixture (11 mL; ratio 4:1) and dropwise treated with tetrabutylammonium fluoride (2.54 mL, 665 mg, 1 M in THF, 2.54 mmol, 1.00 eq.). The reaction mixture was then stirred at 65 °C for 16 h. After cooling the mixture to room temperature, brine (200 mL) was added and the solution was extracted with ethyl acetate (2×200 mL). The combined organic phases were washed with brine (2×200 mL) and dried over Na_2SO_4. The solvent was removed under reduced pressure to give a brown oil which was purified by column chromatography (hexane: ethyl acetate). The product was obtained as a brown solid (718 mg, 1.64 mmol, 65 %).

^{1}H-NMR (400 MHz, $CDCl_3$): δ [ppm] = 9.25 (dd, $^3J_{HH}$ = 4.3, 1.8 Hz, 1H, CH_{Php}), 8.98 (dd, $^3J_{HH}$ = 7.9, 1.1 Hz, 1H, CH_{Py}), 8.90 (d, $^3J_{HH}$ = 8.4 Hz, 1H, CH_{Py}), 8.55(s, 1H, CH_{Tri}), 8.38 (d, $^3J_{HH}$ = 8.4 Hz, 1H, CH_{Php}), 8.26 (ddd, $^3J_{HH}$ = 7.8, 2.9, 1.5 Hz, 2H, CH_{Php}), 8.01 (t, $^3J_{HH}$ = 7.8 Hz, 1H, CH_{Php}), 7.82 (m, 2H, CH_{Php}), 7.65 (dd , $^3J_{HH}$ = 8.0, 4.3 Hz, 1H, CH_{Py}), 6.35 (s, 2H, CH_2), 1.22 (s, 9H, tBu).

$^{13}C^{1}H$ NMR (101 MHZ, $CDCl_3$): δ [ppm] = 178.0 (C_q), 156.0 (C-C_q), 155.9 (C_q), 150.6 (CH_{Php}), 149.3 (C_q), 149.2 (C_q), 146.5 (C_q), 145.8 (C_q), 138.1 (CH_{Php}), 137.0 (CH_{Php}), 136.4 (CH_{Php}), 129.2 (C_q), 129-0 (C_q), 127.0 (CH_{Php}), 126.7 (CH_{Php}), 123.7 (CH_{Tri}), 123.1 (CH_{Py}), 122.3 (CH_{Py}), 121.3 (CH_{Py}), 120.9 (CH_{Php}), 69.9 (CH_2), 39.0 (C_q), 27.0 (CH_3).

IR (ATR): $\bar{\nu}$ [cm^{-1}] = 3112 (vw), 2974 (vw), 2932 (vw), 2871 (vw), 1745 (w), 1600 (vw), 1557 (vw), 1505 (vw), 1492 (vw), 1457 (vw), 1439 (vw), 1411 (w), 1367 (vw), 1276 (w), 1256 (w), 1187 (vw), 1121 (m), 1061 (vw), 1033 (w), 1015 (w), 991 (w), 943 (vw), 884 (vw), 867 (w), 828 (w), 796 (w), 772 (w), 747 (w), 720 (w), 681 (vw), 657 (vw), 645 (vw), 623 (vw), 579 (vw), 531 (vw), 509 (vw), 484 (vw), 448 (vw), 418 (vw).

ESI-MS [m/z] ($C_{25}H_{23}N_6O_2$, $[M+H]^+$): calc. 439.18, found 439.18.

1.2 $[Er(PPTMP)_2(H_2O)][OTf]_3$

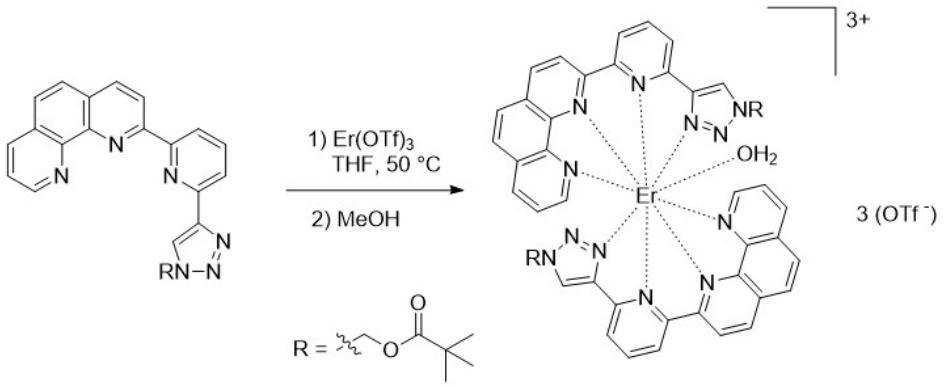

Figure S2: Synthesis scheme of complex **1**.

PPTMP (100 mg, 0.228 mmol, 1.00 eq.) and erbium(III) trifluoromethanesulfonate (140 mg, 0.288 mmol, 1.00 eq.) were dissolved in THF (10 mL) and heated overnight at 50 °C resulting in the formation of a pink precipitate. The supernatant was decanted and the precipitate was dried under vacuum. The precipitate was dissolved in hot methanol and the solution was allowed to evaporate slowly at room temperature. After a few days, pink crystals of the product were obtained. Yield: 53 mg, 34.4 mmol, 15 %

IR (ATR): $\bar{\nu}$ [cm^{-1}] = 3392 (m), 3257 (w), 2924 (vw), 2853 (vw), 1743 (vw), 1659 (w), 1642 (w), 1627 (w), 1576 (vw), 1523 (vw), 1499 (vw), 1476 (vw), 1431 (vw), 1391 (vw), 1223 (s), 1180 (m), 1082 (vw), 1025 (s), 859 (vw), 829 (vw), 808 (vw), 770 (vw), 746 (vw), 669 (vw), 631 (m), 577 (vw), 517 (w).

ESI-MS [m/z] ($C_{52}H_{44}ErF_6N_{12}O_{10}S_2$, $[M–OTf\text{-}H_2O]^+$): calc. 1342.20, found. 1342.19.

2 Crystal Structure

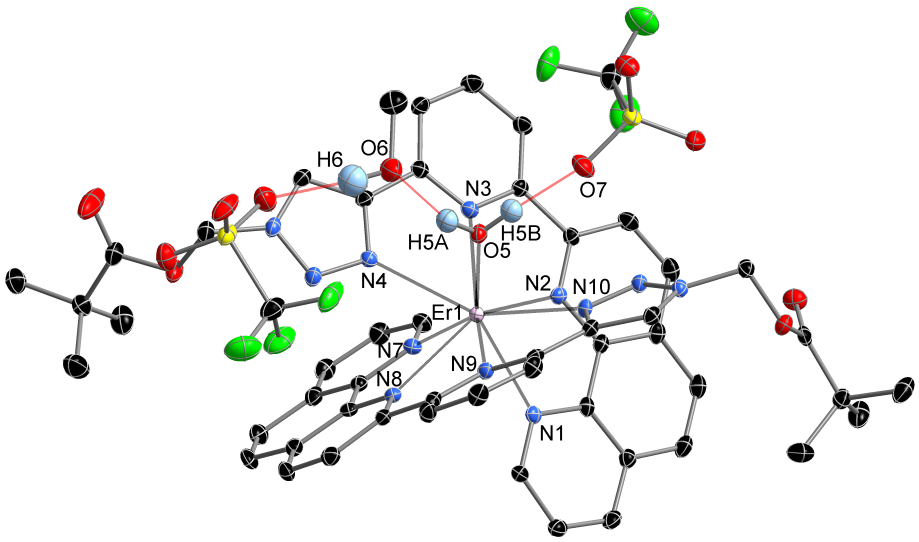

Figure S3: Molecular structures of $[Er(PPTMP)_2(H_2O)][OTf]_3$ in the solid state. Hydrogen atoms, solvent molecules, and uncoordinated triflate ions are omitted for the sake of clarity. Thermal ellipsoids are drawn at 50 % probability. Only selected hydrogen atoms are shown for clarity. Selected bond lengths (Å) and angles (°): Er1-N1 2.507(2), Er1-N2 2.473(2), Er1-N3 2.508(2), Er1-N4 2.529(2), Er1-N7 2.481(2), Er1-N8 2.473(2), Er1-N9 2.510(2), Er1-N10 2.4956(19), Er1-O5 2.3550(16), H5A-O6 1.8151(21), H5B-O7 1.8596(21), H6-O10 1.9191(23), N1-Er1-N2 66.54(7), N2-Er1-N3 63.67(7), N3-Er1-N4 65.39(7), N7-Er1-N8 66.68(7), N8-Er1-N9 63.45(7), N9-Er1-N10 65.43(7).

Table S1: Crystal data, data collection and refinement of compound $[Er(PPTMP)_2(H_2O)][OTf]_3$.

Compounds	$[Er(PPTMP)_2(H_2O)][OTf]_3$
Chemical formula	$C_{54}H_{50}ErF_9N_{12}O_{15}S_3$
CCDC Number	2472872
Formula Mass	1541.50
Radiation type	MoK_α
Wavelength/nm	0.71073
Crystal system	triclinic
a/Å	12.1106(4)
b/Å	13.8842(5)
c/Å	18.2897(7)
$\alpha/^\circ$	83.778(3)
$\beta/^\circ$	82.542(3)
$\gamma/^\circ$	84.534(3)
Unit cell volume/Å^3	3021.07(2)
Temperature/K	100
Space group	$P\bar{1}$
Z	2
Absorption coefficient, μ/mm	1.598
No. of reflections measured	40840
No. of independent reflections	15900
R_{int}	0.0303
Final R_1 values ($I > 2\sigma(I)$)	0.0324
Final $wR(F^2)$ values ($I > 2\sigma(I)$)	0.0722
Final R_1 values (all data)	0.0442
Final $wR(F^2)$ values (all data)	0.0756
Goodness of fit on F^2	0.985

3 NMR Spectroscopy

NMR spectra were recorded on Bruker spectrometers (Avance Neo 300 MHz, Avance Neo 400 MHz or Avance III 400 mHz). All NMR spectra were measured at 298 K, unless otherwise specified. The multiplicity of the signals is indicated as s = singlet, d = doublet, dd = doublet of doublets, t = triplet, q = quartet, m = multiplet and br = broad.

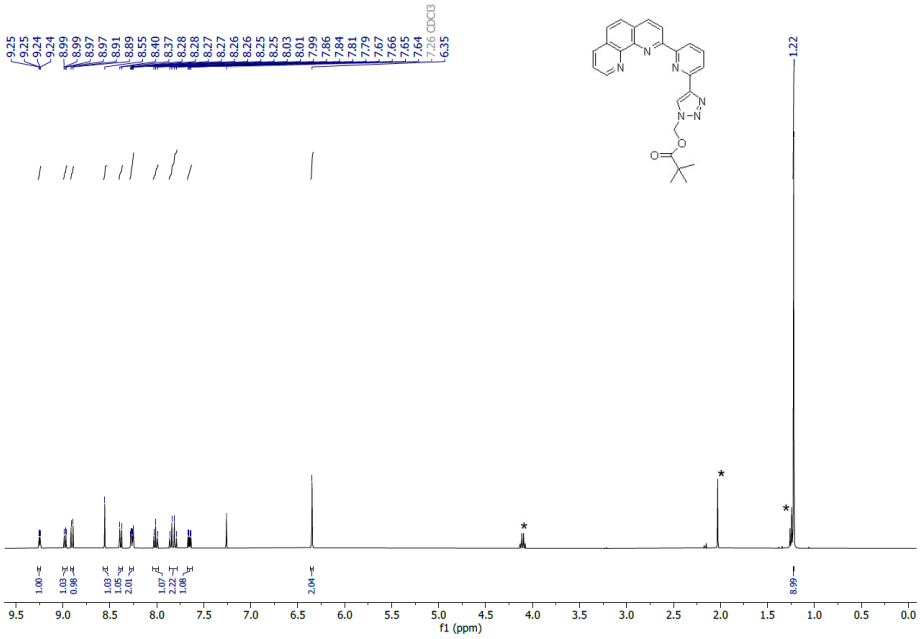

Figure S4: ^{1}H NMR spectrum (400 mHz, $CDCl_3$, 298 K) of (4-(6-(1,10-phenanthrolin-2-yl)pyridin-2-yl)-1H-1,2,3-triazol-1-yl)methyl pivalate (PPTMP). *Solvent signal.

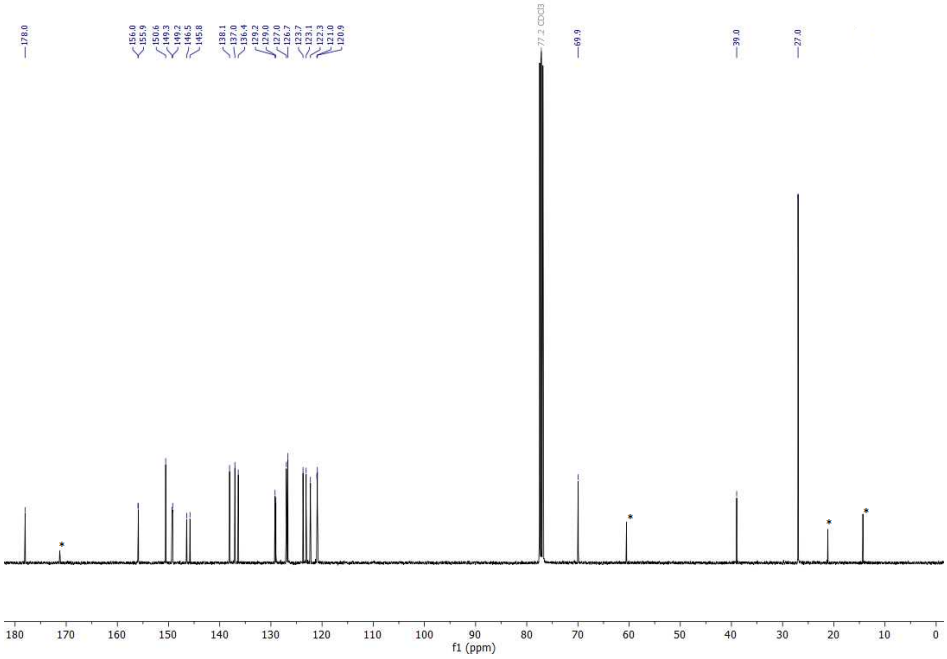

Figure S5: $^{13}C^{1}H$ NMR spectrum (400 mHz, $CDCl_3$, 298 K) of PPTMP. *Solvent signal.

4 IR Spectroscopy

Infrared (IR) spectra were recorded in the region 4000–400 cm-1 on a Bruker Tensor 37 FTIR spectrometer equipped with a room temperature DLaTGS detector, a diamond attenuated total reflection (ATR) unit and a nitrogen-flushed chamber. In terms of their intensity, the signals were classified into different categories (vs = very strong, s = strong, m = medium, w = weak, and sh = shoulder).

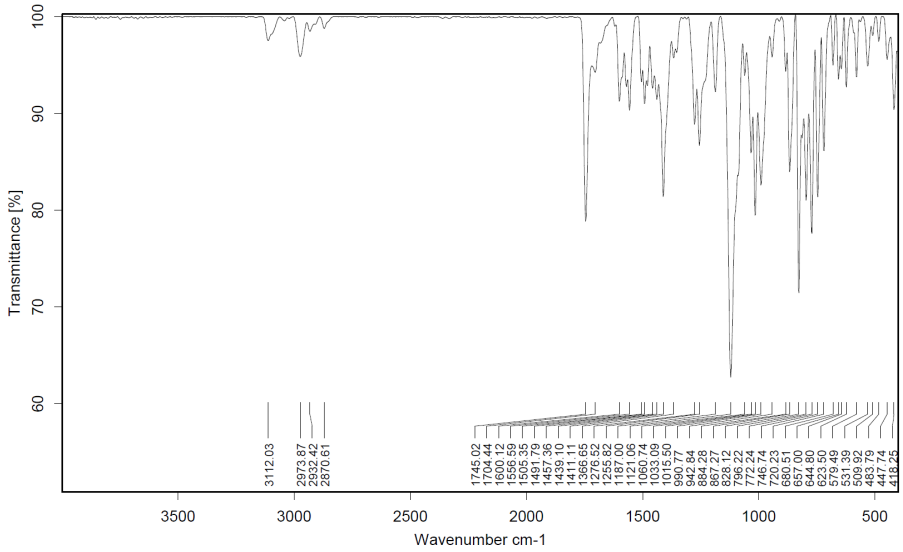

Figure S6: IR spectrum of PPTMP

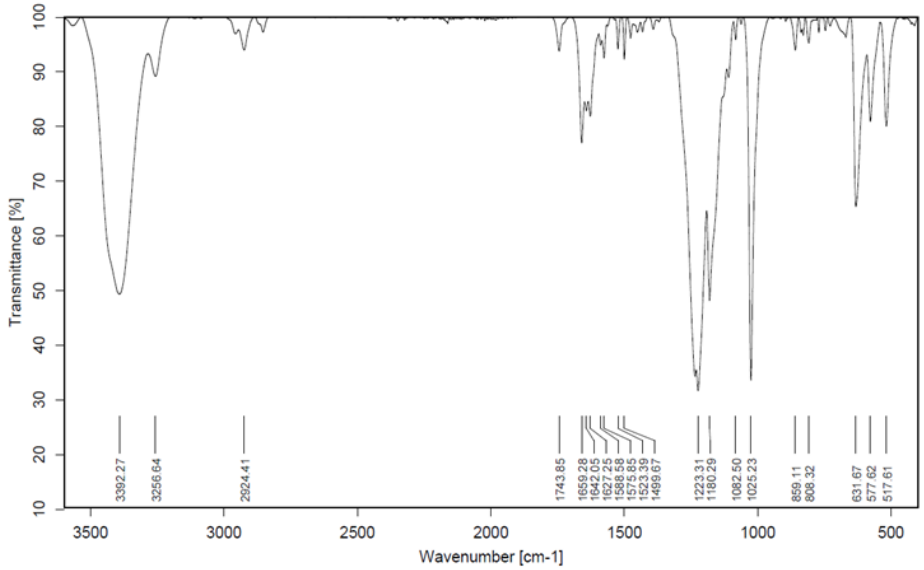

Figure S7: IR spectrum of $[Er(PPTMP)_2(H_2O)][OTf]_3$.

5 Mass Spectrometry

MS spectra were obtained on a Thermo Fisher Scientific LTQ Orbitrap XLQ Exactive mass spectrometer.

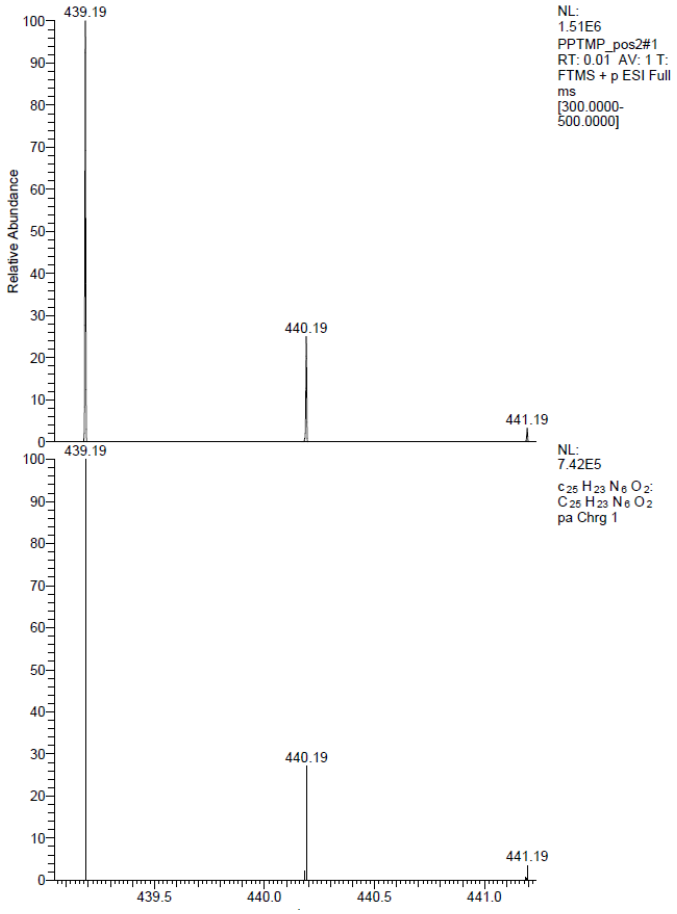

Figure S8: MS-ESI spectra of PPTMP. Shown is the molecular ion Peak $[M+H]^+$. Top: experimental spectrum, Bottom: simulated signals.

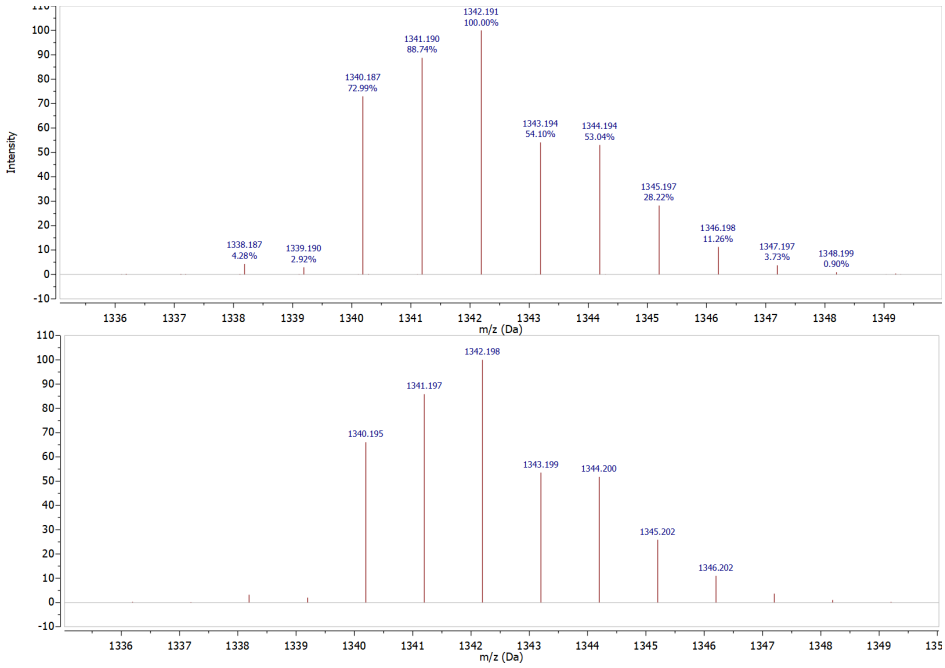

Figure S9: MS-ESI spectra of $[Er(PPTMP)_2(H_2O)][OTf]_3$. Shown is the molecular ion Peak [M – OTf-H_2O]$^+$. Top: experimental spectrum, Bottom: simulated signals.

6 Magnetic Susceptibility

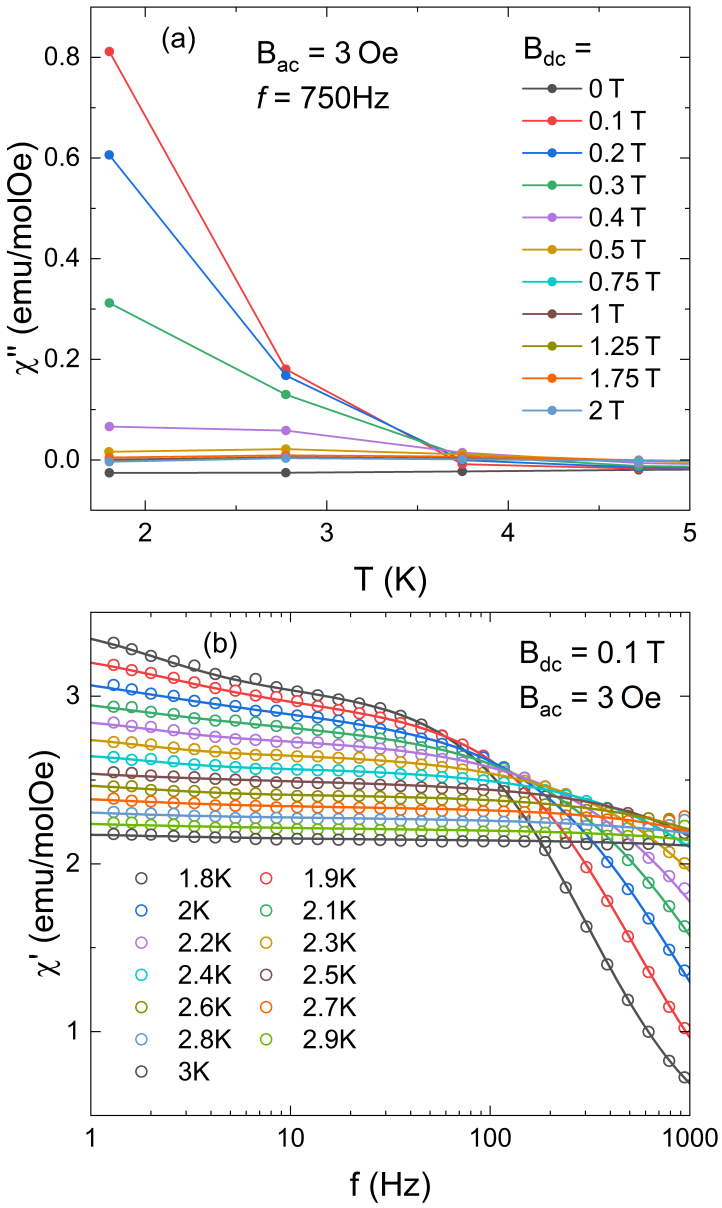

Figure S10: (a) Temperature dependence of the out-of-phase susceptibility at $f = 750$ Hz and various static magnetic fields. (b) Frequency dependence of the in-phase susceptibility at various temperatures. Solid lines depict fits of eq. (1) to the data.

Table S2: Relaxation times τ_{i} and distribution parameters α_{i} obtained by fitting the experimental ac susceptibility data using eq. (1) at different temperatures as described in the main text.

T (K)	τ_1 (s)	α_1	τ_2 (ms)	α_2
1.8	0.49	0.1	3.2	0.15
1.9	0.45	0.22	1.9	0.19
2.0	0.68	0.35	1.1	0.24
2.1	0.75	0.26	7.05×10^{-1}	0.28
2.2	0.54	0.02	5.64×10^{-1}	0.3
2.3	0.59	0	2.82×10^{-1}	0.3
2.4	0.55	0	1.36×10^{-1}	0.3
2.5	0.66	0.13	9.18×10^{-2}	0.28
2.6	1.13	0.27	8.19×10^{-3}	0.29
2.7	0.69	0.15	4.99×10^{-3}	0.28
2.8	3.09	0.33	2.38×10^{-3}	0.29
2.9	2.16	0.49	5.02×10^{-2}	0.23
3.0	0.70	0.37	2.84×10^{-3}	0.21

7 HF-EPR spectroscopy

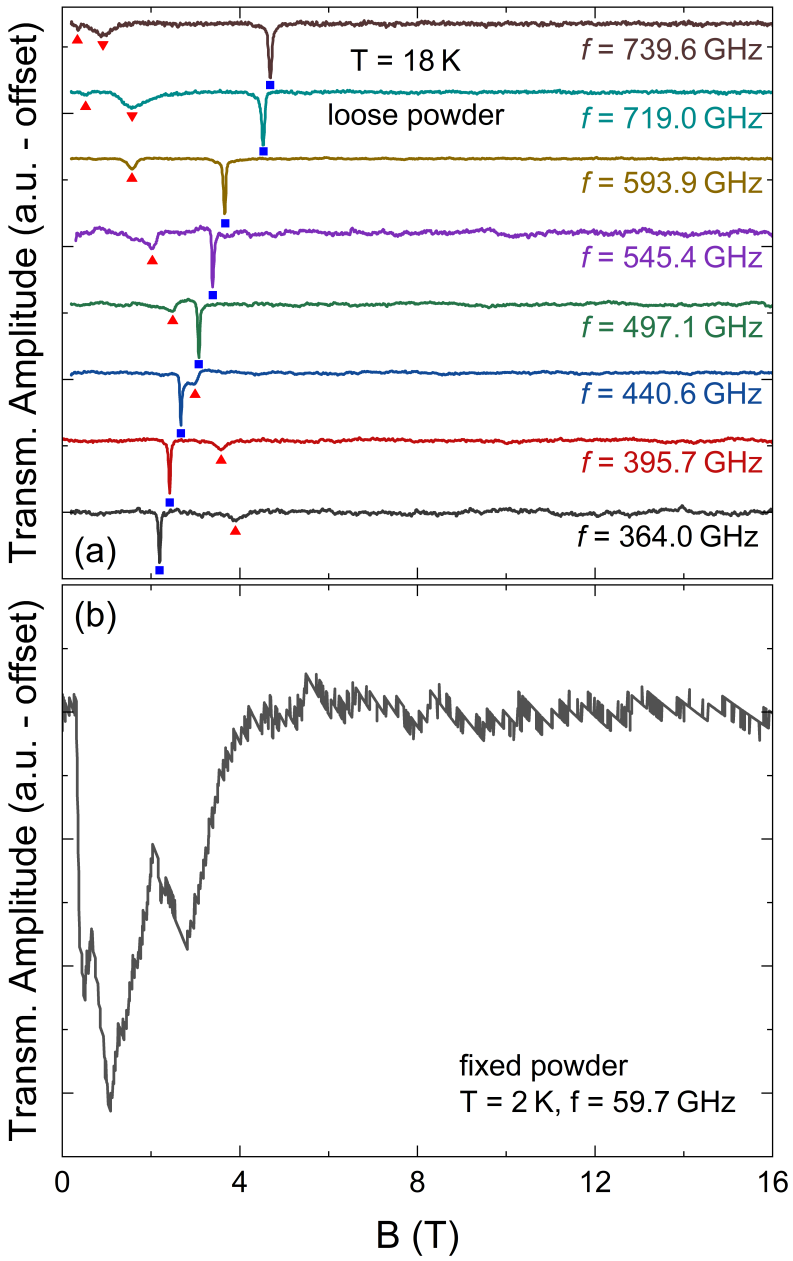

Figure S11: (a) Loose powder HF-EPR spectra up to 16 T for various microwave frequencies measured at $T = 18$ K. Symbols mark resonance field positions as colour-coded in the main text. (b) Fixed powder HF-EPR spectrum at $f = 59.7$ GHz and $T = 2$ K up to 16 T.

8 Calculations

In the following the multistep procedure to obtain reliable starting orbitals for CASOCI is explained: For all computationally investigated models, Y is replaced to Gd and an unrestricted Kohn Sham calculation is performed using the B3-LYP functional, the all-electron basis x2c-TZVPall for Gd, the def2-TZVP basis for the remaining atoms and an energy convergence criterium of 10^{-7} E_h. Scalar relativistic effects are accounted for using X2C.[2] The half filled natural orbitals of this calculation are used as a starting point for a Restricted Open Shell Hartree Fock (ROHF) calculation on the same compound, now using the second order Douglass Kroll Hess approach to treat scalar relativistic effects.[3,4] We note, that while the choice of relativistic treatment prior to the last step is a cost-accuracy-availability balance, the final CASOCI calculation is always on a DKH4 level of theory. This ensures a reliable starting guess for pure f orbitals in the active space. In a next step, Gd is replaced to Er equipped with a x2c-TZVPall basis and the orbitals of the previous calculation are used as a starting guess. The Roothaan parameters used are $a = 119/121$ and $b = 126/121$ mimicking an average over all quartet states with eleven electrons in the seven $4f$ orbitals for the orbital optimization. In a last step DKH2 is changed to DKH4 and a density convergence criterium of 10^{-7} is introduced keeping the energy convergence criterium of 10^{-7} E_h for a tight convergence of the calculation.

Table S3: Energies of the lowest $^4I_{15/2}$-ground state multiplet of compound **1** using the bare molecule as a model cluster.

energy in cm^{-1}	g_x	g_y	g_z
0	0.464113	1.33494	12.07135
24.604	1.78109	3.394893	11.94594
86.201	6.276628	4.488298	0.852313
117.686	0.95098	1.205286	13.8677
190.68	1.115064	1.635626	9.377779
232.198	1.893061	4.617316	8.263319
287.281	3.13556	3.820199	8.460835
329.869	1.521774	3.034892	13.18099

Table S4: Energies of the lowest $^4I_{15/2}$-ground state multiplet of compound **1** using the bare molecule and the MeOH molecule H-bonded to it as a model cluster.

energy in cm^{-1}	g_x	g_y	g_z
0	0.742199	1.545679	12.48478
21.835	0.911138	4.124384	11.71255
91.338	6.216954	3.589997	0.462906
113.683	0.802401	1.155125	13.81597
190.721	0.690271	1.958725	10.79499
235.934	0.027568	2.476183	7.318452
291.169	4.84864	5.098171	6.745822
323.111	2.722719	3.698815	11.52246

Table S5: Energies of the lowest $^4I_{15/2}$-ground state multiplet of compound **1** using the bare molecule and the MeOH molecule H-bonded to it as well as the closest triflate ion as a model cluster.

energy in cm^{-1}	g_x	g_y	g_z
0	1.631398	2.705136	12.22968
23.107	0.956058	2.769475	9.756338
103.512	4.982802	3.466588	1.53308
118.033	0.692166	0.780354	12.04524
195.933	0.33995	1.526324	12.04844
244.904	5.789047	4.055977	1.125247
302.132	0.905727	3.873352	11.07073
328.556	4.052207	5.512911	8.931604

Table S6: Energies of the lowest $^4I_{15/2}$-ground state multiplet of compound **1** using the bare molecule and the MeOH molecule H-bonded to it as well as the two closest triflate ionas a model cluster.

energy in cm^{-1}	g_x	g_y	g_z
0	1.113272	1.979091	12.5744
25.433	0.905556	1.705587	9.41756
108.156	2.146888	2.454909	5.191053
121.53	0.674756	0.853468	11.74836
198.558	0.209542	1.164288	12.33081
249.111	5.480398	4.099915	1.058192
304.159	0.565985	2.857098	12.21493
332.622	3.407895	5.381822	9.798135

Table S7: Energies of the lowest $^4I_{15/2}$-ground state multiplet of compound **1** using the bare molecule and the MeOH molecule H-bonded to it as well as the three closest triflate ion as a model cluster.

energy in cm^{-1}	g_x	g_y	g_z
0	1.099575	1.954822	12.61568
26.275	0.552248	1.986302	9.15806
109.434	2.115618	2.258052	5.415104
122.846	0.751401	0.80461	11.43809
199.488	0.246097	1.114088	12.42371
250.93	5.330429	4.102663	0.857963
304.309	0.536737	2.562988	12.50193
334.148	3.197615	5.552147	9.932153

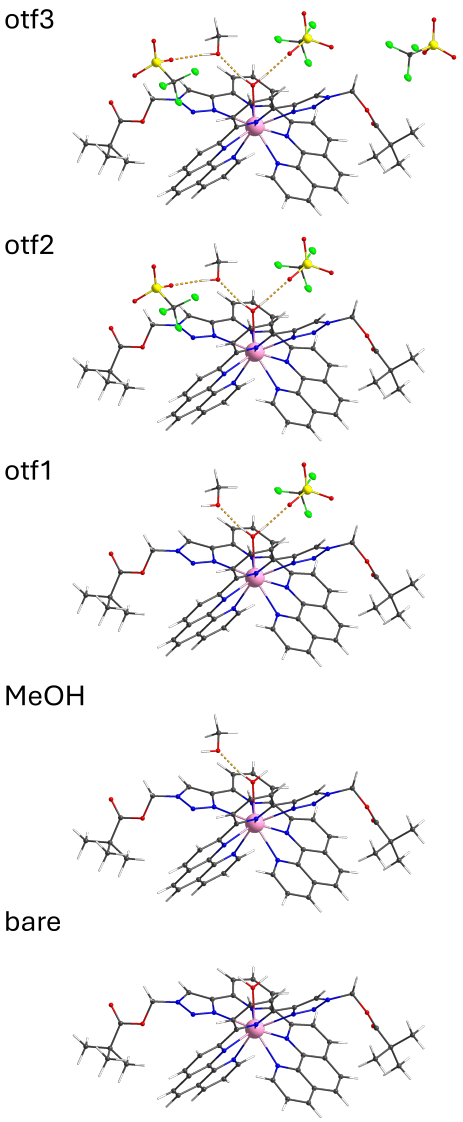

Figure S12: A representation of the five models used in this study. The otf3 model is charge neutral and contains three triflate anions. For the model otf2, the triflate furthest from the Er-centre is removed, leaving a mono-cationic complex. Next, the triflate which is H-bonded to the methanol molecule is removed, leaving a di-cationic complex otf1. In the fourth calculation, the last triflate anion is removed and the complex has a charge +3 and is named MeOH. Finally, the MeOH molecule is removed as well leaving only the PPTMP ligand and keeping the charge of +3. This model is called bare.

Table S8: Energies of the lowest $^4I_{15/2}$-ground state multiplet of compound **1** using the bare molecule as a model cluster. A CASSCF optimization was carried out between the ROHF and CASOCI step.

energy in cm^{-1}	g_x	g_y	g_z
0	0.437315	1.224908	12.14806
25.33	1.705553	3.337955	11.90137
86.709	6.264674	4.482181	0.724821
118.019	0.951084	1.243748	13.78266
190.987	1.110709	1.638579	9.502643
233.377	1.897018	4.637909	8.1871
288.522	3.285838	3.769121	8.383363
330.262	1.571389	3.141852	13.07045

Table S9: Energies of the lowest $^4I_{15/2}$-ground state multiplet of compound **1** using the bare molecule and the MeOH molecule H-bonded to it as a model cluster. A CASSCF optimization was carried out between the ROHF and CASOCI step.

energy in cm^{-1}	g_x	g_y	g_z
0	0.856189	1.526494	12.52223
22.428	0.798786	4.011603	11.66128
92.197	6.247546	3.438501	0.59067
113.384	0.822889	1.219776	13.62486
190.708	0.673073	1.912892	10.97049
236.903	0.052488	2.441664	7.158722
292.189	4.531956	5.517375	6.55688
322.949	2.97856	3.991183	11.0749

Table S10: Energies of the lowest $^4I_{15/2}$-ground state multiplet of compound **1**using the bare molecule and the MeOH molecule H-bonded to it as well as the closest triflate ion as a model cluster. A CASSCF optimization was carried out between the ROHF and CASOCI step.

energy in cm^{-1}	g_x	g_y	g_z
0	1.493303	2.523566	12.36575
24.725	0.837243	2.576931	9.778527
105.373	1.309957	2.966753	5.391502
118.907	0.59904	0.791178	11.15819
196.364	0.340987	1.443163	12.1798
247.391	5.58718	4.28406	1.32184
303.162	0.635504	3.215362	11.95843
331.352	3.686098	5.151231	9.798212

Table S11: Energies of the lowest $^4I_{15/2}$-ground state multiplet of compound **1**using the bare molecule and the MeOH molecule H-bonded to it as well as the two closest triflate ionas a model cluster. A CASSCF optimization was carried out between the ROHF and CASOCI step.

energy in cm^{-1}	g_x	g_y	g_z
0	0.96626	1.729378	12.72756
27.519	0.695202	1.541026	9.43105
110.685	1.450073	2.415749	5.644436
123.261	0.622711	0.832885	10.86447
199.404	0.190473	1.061793	12.47081
252.422	5.250636	4.369285	1.288032
305.547	0.376178	2.301162	12.94375
336.981	2.868193	5.302695	10.58111

Table S12: Energies of the lowest $^4I_{15/2}$-ground state multiplet of compound **1**using the bare molecule as a model cluster. No optimization of H-positions was carried out.

energy in cm^{-1}	g_x	g_y	g_z
0	0.991976	1.510749	11.85706
25.717	1.772279	2.953194	11.74088
86.571	6.170677	4.82162	0.979597
120.133	1.03349	1.249405	13.71368
191.411	0.89937	1.712352	9.45204
233.691	2.029505	4.89248	8.152496
290.152	3.120746	3.417466	8.539775
332.964	1.547915	3.254118	13.0068

Table S13: Energies of the lowest $^4I_{15/2}$-ground state multiplet of compound **1**using the bare molecule and the MeOH molecule H-bonded to it as a model cluster. No optimization of H-positions was carried out.

energy in cm^{-1}	g_x	g_y	g_z
0	0.095125	0.892639	12.42285
23.467	1.389848	3.863905	11.88953
89.222	6.357639	3.923672	0.02646
116.299	0.87636	1.25705	13.73171
190.634	0.84461	1.794934	10.57859
236.396	0.800113	3.358106	7.443024
291.657	4.529407	4.878332	6.943376
326.758	2.283571	3.644	11.99173

Table S14: Energies of the lowest $^4I_{15/2}$-ground state multiplet of compound **1**using the bare molecule and the MeOH molecule H-bonded to it as well as the closest triflate ion as a model cluster. No optimization of H-positions was carried out.

energy in cm^{-1}	g_x	g_y	g_z
0	1.614803	1.865976	12.46999
22.86	0.157326	3.251541	10.70548
98.265	5.460793	3.838279	1.238611
116.995	0.678479	1.117233	13.12727
193.617	0.514259	1.570941	11.80541
243.106	6.201738	3.39482	0.539938
300.819	2.12197	5.222067	8.691719
327.023	7.639326	6.65206	4.028478

Table S15: Energies of the lowest $^4I_{15/2}$-ground state multiplet of compound **1**using the bare molecule and the MeOH molecule H-bonded to it as well as the two closest triflate ionas a model cluster. No optimization of H-positions was carried out.

energy in cm^{-1}	g_x	g_y	g_z
0	1.339302	1.739905	12.59215
24.068	0.605552	2.224844	10.24775
102.075	4.786978	3.49886	2.08559
118.859	0.880616	1.024245	13.20331
195.313	0.39787	1.277172	12.08874
246.24	0.02878	2.964646	5.982694
302.587	1.728306	4.230371	9.76917
328.713	7.170646	6.549741	4.62294

Table S16: Energies of the lowest $^4I_{15/2}$-ground state multiplet of compound **1**using the bare molecule and the MeOH molecule H-bonded to it as well as the three closest triflate ion as a model cluster. No optimization of H-positions was carried out.

energy in cm^{-1}	g_x	g_y	g_z
0	1.328328	1.783609	12.5768
24.455	0.445854	2.339629	9.926323
103.128	4.886424	3.790953	1.789334
119.945	0.750364	1.160636	12.96313
196.235	0.42971	1.200069	12.19569
247.535	5.814669	3.187008	0.010047
303.029	1.555081	3.733499	10.33218
329.973	7.616898	6.248161	4.591696

Table S17: Extended Stevens Operator Equivalents B(k,q) for different models of compound **1**using ROHF to optimize the orbitals.

	bare	MeOH	otf1	otf2	otf3
B(2,-2)	1.391387931E-01	1.471725309E-01	1.095681622E-01	1.361509565E-01	1.007382274E-01
B(2,-1)	-7.317330528E-01	-7.014531087E-01	-6.507781407E-01	-5.050233498E-01	-4.753978122E-01
B(2, 0)	-1.563935728E-03	-1.811445843E-02	-5.939380643E-02	-7.449722337E-02	-8.287648107E-02
B(2, 1)	-5.756200913E-01	4.030153905E-02	7.858176681E-01	9.122341180E-01	9.292325241E-01
B(2, 2)	-2.577715889E-01	-2.438922860E-02	1.880796660E-01	1.642826014E-01	1.402323629E-01
B(4,-4)	2.464661857E-03	2.479978921E-03	2.900623710E-03	2.855724175E-03	2.980857810E-03
B(4,-3)	-5.187147318E-03	-5.329972523E-03	-3.989113282E-03	-5.343696334E-03	-4.765103009E-03
B(4,-2)	2.864366640E-03	3.007335893E-03	3.785291843E-03	3.883190069E-03	4.053989911E-03
B(4,-1)	-3.686727436E-03	-3.645146768E-03	-3.818749612E-03	-3.876087025E-03	-3.946742993E-03
B(4, 0)	-1.561310627E-03	-1.582881570E-03	-1.574482520E-03	-1.597217504E-03	-1.554972825E-03
B(4, 1)	-1.077200822E-02	-1.103490942E-02	-1.062382502E-02	-1.043336077E-02	-1.038856778E-02
B(4, 2)	4.471229684E-03	4.633219638E-03	4.932917731E-03	4.820056585E-03	4.874196131E-03
B(4, 3)	1.143558902E-02	1.360135435E-02	1.611675817E-02	1.682608268E-02	1.711218793E-02
B(4, 4)	-5.494035013E-03	-5.014160908E-03	-4.615736898E-03	-3.970450293E-03	-4.100563475E-03
B(6,-6)	-3.153291213E-05	-4.485535407E-05	-6.767281477E-05	-7.821815746E-05	-8.048390438E-05
B(6,-5)	1.729129924E-03	1.714590124E-03	1.811244559E-03	1.722334656E-03	1.782773184E-03
B(6,-4)	-3.590098293E-04	-3.645941475E-04	-3.620061451E-04	-3.686694417E-04	-3.668822265E-04
B(6,-3)	4.189096310E-04	3.953942358E-04	3.604163606E-04	3.390158577E-04	3.373146298E-04
B(6,-2)	-2.634091073E-04	-2.567700525E-04	-2.402816280E-04	-2.439458946E-04	-2.383037027E-04
B(6,-1)	3.167730154E-04	3.315924688E-04	3.511025902E-04	3.783557445E-04	3.739886895E-04
B(6, 0)	3.605547038E-05	3.720263969E-05	3.888796522E-05	3.890937515E-05	3.943248629E-05
B(6, 1)	-5.222560654E-05	-5.201318971E-05	-5.576681047E-05	-5.803390582E-05	-5.766943125E-05
B(6, 2)	-2.777859272E-04	-2.816999918E-04	-2.811057846E-04	-2.871258141E-04	-2.850192137E-04
B(6, 3)	6.069686102E-04	6.030638898E-04	6.175649856E-04	6.152729208E-04	6.167467003E-04
B(6, 4)	5.117310144E-05	4.118662834E-05	1.739330393E-05	8.249773350E-06	4.765798082E-06
B(6, 5)	-1.156586170E-04	-1.669756630E-04	-3.707975602E-04	-4.148990733E-04	-4.476168398E-04
B(6, 6)	1.664629109E-04	1.670298560E-04	1.450479113E-04	1.490783976E-04	1.407551883E-04
B(8,-8)	1.545258468E-08	1.636824995E-08	1.595600251E-08	1.637877235E-08	1.605534613E-08
B(8,-7)	-1.782808010E-08	-1.137962137E-08	-8.439832137E-10	-5.393098409E-09	-3.768599095E-09
B(8,-6)	-7.593833606E-09	-7.806865911E-09	-7.672632190E-09	-7.495327215E-09	-7.586122715E-09
B(8,-5)	-4.652515620E-08	-4.718219000E-08	-5.259876801E-08	-5.060322851E-08	-5.336163241E-08
B(8,-4)	-1.366662765E-08	-1.402190770E-08	-1.637919979E-08	-1.497117533E-08	-1.619108702E-08
B(8,-3)	-3.559754698E-08	-3.736359334E-08	-4.956826973E-08	-4.686765304E-08	-4.924346283E-08
B(8,-2)	-7.883689701E-10	-7.867133612E-09	-1.696034288E-08	-1.711544582E-08	-1.733584573E-08
B(8,-1)	8.955458594E-11	2.054767215E-09	3.938586809E-09	3.507151480E-09	3.269353052E-09
B(8, 0)	5.553953168E-10	5.646684146E-10	6.421775836E-10	6.509963022E-10	6.604753092E-10
B(8, 1)	-4.251213801E-09	-1.146458902E-09	2.631325953E-09	3.312236231E-09	3.576480681E-09
B(8, 2)	-4.224774361E-09	-5.765977245E-09	-5.028138078E-09	-5.052743560E-09	-4.473821287E-09
B(8, 3)	-4.742325566E-08	-4.533858357E-08	-4.160339940E-08	-3.226923969E-08	-3.468916841E-08
B(8, 4)	-2.393968587E-08	-2.173144638E-08	-1.843708840E-08	-1.967696749E-08	-1.965637171E-08
B(8, 5)	1.263044680E-08	1.101630984E-08	1.066891977E-08	1.691337528E-08	1.752795805E-08
B(8, 6)	2.371421307E-08	2.467738966E-08	2.523056487E-08	2.509560399E-08	2.489102383E-08
B(8, 7)	-7.365723795E-08	-7.366664938E-08	-7.688628896E-08	-8.032769695E-08	-8.073694572E-08
B(8, 8)	-2.954651783E-08	-2.893546432E-08	-2.918349226E-08	-2.932420579E-08	-2.949452050E-08

Table S18: Extended Stevens Operator Equivalents B(k,q) for different models of compound **1**using ROHF and CASSCF to optimize the orbitals.

	bare	MeOH	otf1	otf2
B(2,-2)	1.439020816E-01	1.427131875E-01	1.043011046E-01	1.317047797E-01
B(2,-1)	-7.381846977E-01	-7.049115386E-01	-6.612618482E-01	-5.049609665E-01
B(2, 0)	-8.775700956E-03	-2.646070967E-02	-6.947920827E-02	-8.754914210E-02
B(2, 1)	-5.566424875E-01	9.795527777E-02	8.940958819E-01	1.031519519E+00
B(2, 2)	-2.692282033E-01	-2.506149270E-02	1.950575866E-01	1.670297763E-01
B(4,-4)	2.517640742E-03	2.514193168E-03	2.933976884E-03	2.899342142E-03
B(4,-3)	-5.196454121E-03	-5.391131586E-03	-4.118753263E-03	-5.368125346E-03
B(4,-2)	2.859236867E-03	3.005201431E-03	3.803942610E-03	3.930378722E-03
B(4,-1)	-3.710766818E-03	-3.669453784E-03	-3.843312160E-03	-3.923544641E-03
B(4, 0)	-1.577920431E-03	-1.592205321E-03	-1.580402023E-03	-1.609946244E-03
B(4, 1)	-1.084122905E-02	-1.111597059E-02	-1.069356464E-02	-1.052660052E-02
B(4, 2)	4.513162734E-03	4.673482334E-03	4.990953542E-03	4.905085381E-03
B(4, 3)	1.136431016E-02	1.365442408E-02	1.614380978E-02	1.700547057E-02
B(4, 4)	-5.509890799E-03	-5.047735706E-03	-4.655739690E-03	-3.966080252E-03
B(6,-6)	-3.257239042E-05	-4.670750372E-05	-6.892294228E-05	-8.031040685E-05
B(6,-5)	1.735581972E-03	1.717872409E-03	1.818895855E-03	1.726082225E-03
B(6,-4)	-3.593667460E-04	-3.644790231E-04	-3.616390645E-04	-3.674476376E-04
B(6,-3)	4.127782809E-04	3.911553992E-04	3.564827025E-04	3.328487336E-04
B(6,-2)	-2.640644418E-04	-2.562959365E-04	-2.405935463E-04	-2.436481798E-04
B(6,-1)	3.213695373E-04	3.337268704E-04	3.543063801E-04	3.830724831E-04
B(6, 0)	3.570507397E-05	3.710559163E-05	3.889770770E-05	3.918405657E-05
B(6, 1)	-5.559288353E-05	-5.239066265E-05	-5.752010045E-05	-5.931376894E-05
B(6, 2)	-2.791233628E-04	-2.822747461E-04	-2.815329776E-04	-2.889394017E-04
B(6, 3)	6.065857473E-04	6.025281860E-04	6.171983316E-04	6.186305306E-04
B(6, 4)	5.010767074E-05	4.099992188E-05	1.753034470E-05	7.688832909E-06
B(6, 5)	-1.228727593E-04	-1.716242533E-04	-3.781957841E-04	-4.306128452E-04
B(6, 6)	1.664793563E-04	1.659619873E-04	1.439421241E-04	1.487510890E-04
B(8,-8)	1.442025508E-08	1.514733280E-08	1.480906183E-08	1.513828632E-08
B(8,-7)	-1.820357583E-08	-1.064933266E-08	8.507782132E-11	-5.985800232E-09
B(8,-6)	-7.518793359E-09	-7.731237453E-09	-7.427352349E-09	-7.167702690E-09
B(8,-5)	-3.434894803E-08	-3.556138471E-08	-4.185872863E-08	-3.976357791E-08
B(8,-4)	-1.394972072E-08	-1.429061028E-08	-1.656469180E-08	-1.523944100E-08
B(8,-3)	-2.836880898E-08	-3.086110162E-08	-4.308282621E-08	-4.023654402E-08
B(8,-2)	1.154615445E-10	-7.488968019E-09	-1.682032457E-08	-1.674498547E-08
B(8,-1)	3.772614718E-11	2.083657949E-09	4.038584881E-09	3.522272696E-09
B(8, 0)	5.561100334E-10	5.627014141E-10	6.479925062E-10	6.563931144E-10
B(8, 1)	-4.287453957E-09	-9.196019999E-10	3.016518581E-09	3.828049752E-09
B(8, 2)	-4.716556486E-09	-6.188576787E-09	-5.631446394E-09	-5.515007260E-09
B(8, 3)	-4.377690841E-08	-4.291291894E-08	-3.924981605E-08	-2.983732999E-08
B(8, 4)	-2.345381575E-08	-2.080908826E-08	-1.703775292E-08	-1.825728763E-08
B(8, 5)	1.013448192E-08	8.278087470E-09	7.553436793E-09	1.216376168E-08
B(8, 6)	2.254963090E-08	2.338263514E-08	2.375622888E-08	2.352575915E-08
B(8, 7)	-6.775200411E-08	-6.884357787E-08	-7.120423021E-08	-7.570582478E-08
B(8, 8)	-2.693493940E-08	-2.638254051E-08	-2.672477419E-08	-2.674020318E-08

Table S19: Extended Stevens Operator Equivalents B(k,q) for different models of compound **1**using ROHF to optimize the orbitals. Here hydrogen positions were not optimized.

	bare	MeOH	otf1	otf2	otf3
B(2,-2)	9.345294641E-02	1.039931847E-01	4.035771658E-02	6.655263552E-02	2.969456547E-02
B(2,-1)	-7.671929718E-01	-7.432301943E-01	-7.384871748E-01	-5.879883760E-01	-5.625276136E-01
B(2, 0)	-2.456185928E-02	-2.966972683E-02	-7.921615533E-02	-9.113271509E-02	-1.002170586E-01
B(2, 1)	-6.669690808E-01	-1.812671118E-01	4.262971475E-01	5.150471542E-01	5.310993426E-01
B(2, 2)	-2.950345073E-01	-1.191196373E-01	5.958525961E-02	1.831547646E-02	-4.105112518E-03
B(4,-4)	2.304157480E-03	2.338945416E-03	2.685367304E-03	2.651709547E-03	2.763253036E-03
B(4,-3)	-5.790439069E-03	-5.739307336E-03	-4.694187363E-03	-5.988774345E-03	-5.435210626E-03
B(4,-2)	2.661114626E-03	2.784265186E-03	3.472261067E-03	3.570296797E-03	3.734028522E-03
B(4,-1)	-3.724266877E-03	-3.710151246E-03	-3.880158411E-03	-3.940398146E-03	-4.009654310E-03
B(4, 0)	-1.593695114E-03	-1.610787127E-03	-1.587405068E-03	-1.611863866E-03	-1.568430786E-03
B(4, 1)	-1.112169383E-02	-1.129300424E-02	-1.092116468E-02	-1.072818435E-02	-1.067859529E-02
B(4, 2)	4.557298734E-03	4.685078882E-03	4.922695077E-03	4.808646956E-03	4.859645140E-03
B(4, 3)	1.137279327E-02	1.296276684E-02	1.524866352E-02	1.580093552E-02	1.609854792E-02
B(4, 4)	-5.706872099E-03	-5.374921099E-03	-5.038834181E-03	-4.429070427E-03	-4.549619394E-03
B(6,-6)	-3.260696993E-05	-4.195543879E-05	-6.377172874E-05	-7.312152301E-05	-7.554118442E-05
B(6,-5)	1.716171266E-03	1.708318667E-03	1.804940457E-03	1.714864268E-03	1.775731288E-03
B(6,-4)	-3.617478134E-04	-3.652099876E-04	-3.649224453E-04	-3.708644710E-04	-3.692487161E-04
B(6,-3)	4.214230901E-04	4.028426269E-04	3.686820997E-04	3.491024975E-04	3.474279773E-04
B(6,-2)	-2.634985957E-04	-2.587691432E-04	-2.424569420E-04	-2.467214685E-04	-2.411027268E-04
B(6,-1)	3.117543407E-04	3.241774877E-04	3.406820193E-04	3.677461504E-04	3.632857252E-04
B(6, 0)	3.661744881E-05	3.752024295E-05	3.924168452E-05	3.920399585E-05	3.974054323E-05
B(6, 1)	-5.834638204E-05	-5.881849637E-05	-6.198668791E-05	-6.442797704E-05	-6.411549715E-05
B(6, 2)	-2.847758118E-04	-2.871711029E-04	-2.869766818E-04	-2.928549570E-04	-2.908178565E-04
B(6, 3)	6.061306948E-04	6.036044415E-04	6.168044931E-04	6.141918155E-04	6.159490755E-04
B(6, 4)	5.979191704E-05	5.088503920E-05	2.954194387E-05	2.070036974E-05	1.731607452E-05
B(6, 5)	-8.606559347E-05	-1.308508938E-04	-3.167375151E-04	-3.565214114E-04	-3.890931129E-04
B(6, 6)	1.666926342E-04	1.658720998E-04	1.454325199E-04	1.496156527E-04	1.413832060E-04
B(8,-8)	1.542256126E-08	1.608537884E-08	1.569887879E-08	1.610145123E-08	1.578261849E-08
B(8,-7)	-1.893835257E-08	-1.396058870E-08	-4.724102369E-09	-9.320637786E-09	-7.940303278E-09
B(8,-6)	-8.102542163E-09	-8.135468896E-09	-8.230120976E-09	-7.932891932E-09	-8.052740534E-09
B(8,-5)	-4.949873808E-08	-4.975637315E-08	-5.632743082E-08	-5.394897053E-08	-5.666322113E-08
B(8,-4)	-1.334393724E-08	-1.382637089E-08	-1.551013022E-08	-1.408022816E-08	-1.516527188E-08
B(8,-3)	-3.472632890E-08	-3.526682643E-08	-4.664762899E-08	-4.273129064E-08	-4.540685974E-08
B(8,-2)	1.040005024E-09	-4.676386148E-09	-1.245125586E-08	-1.208207664E-08	-1.238109551E-08
B(8,-1)	-3.377266173E-10	1.209177262E-09	2.658786253E-09	2.042976652E-09	1.830399377E-09
B(8, 0)	5.595976764E-10	5.734312054E-10	6.638558450E-10	6.769115683E-10	6.871708839E-10
B(8, 1)	-4.483095606E-09	-2.048810794E-09	1.194431485E-09	1.699787898E-09	1.945939754E-09
B(8, 2)	-4.789026345E-09	-6.139204686E-09	-4.659883280E-09	-4.651788038E-09	-4.073980784E-09
B(8, 3)	-5.350151217E-08	-5.096976110E-08	-5.149589693E-08	-4.248997155E-08	-4.516132292E-08
B(8, 4)	-2.392104718E-08	-2.226386610E-08	-1.927414594E-08	-2.088328805E-08	-2.083613626E-08
B(8, 5)	1.295579890E-08	1.211850572E-08	1.203812117E-08	1.851868729E-08	1.909810988E-08
B(8, 6)	2.341215918E-08	2.422253310E-08	2.472379287E-08	2.456917765E-08	2.438046698E-08
B(8, 7)	-7.413266596E-08	-7.387258254E-08	-7.566965208E-08	-7.923040583E-08	-7.927463936E-08
B(8, 8)	-2.953093950E-08	-2.912071471E-08	-2.919271388E-08	-2.946361750E-08	-2.954262239E-08

Table S20: $m_J(z)$ composition of the lowest 8 Kramers Doublets for compound **1**using the bare molecule as the model compound. Orbitals are optimized with ROHF.

$m_J(z)$	KD1	KD2	KD3	KD4	KD5	KD6	KD7	KD8
+-7.5	0.287	0.021	0.003	0.072	0.354	0.132	0.027	0.103
+-6.5	0.118	0.022	0.024	0.372	0.022	0.221	0.071	0.15
+-5.5	0.025	0.03	0.259	0.347	0.072	0.025	0.178	0.064
+-4.5	0.315	0.055	0.094	0.07	0.117	0.03	0.253	0.065
+-3.5	0.047	0.232	0.356	0.032	0.015	0.045	0.059	0.214
+-2.5	0.172	0.146	0.081	0.018	0.305	0.059	0.05	0.168
+-1.5	0.027	0.239	0.14	0.049	0.091	0.058	0.315	0.082
+-0.5	0.009	0.254	0.042	0.041	0.024	0.429	0.047	0.154

Table S21: $m_J(z)$ composition of the lowest 8 Kramers Doublets for compound **1**using the bare molecule and the MeOH molecule hydrogen bonded to it as the model compound. Orbitals are optimized with ROHF.

$m_J(z)$	KD1	KD2	KD3	KD4	KD5	KD6	KD7	KD8
+-7.5	0.323	0.014	0.001	0.047	0.393	0.089	0.032	0.101
+-6.5	0.091	0.043	0.028	0.461	0.015	0.215	0.014	0.134
+-5.5	0.059	0.011	0.272	0.348	0.05	0.077	0.08	0.104
+-4.5	0.312	0.086	0.044	0.038	0.148	0.061	0.264	0.046
+-3.5	0.04	0.189	0.4	0.017	0.025	0.035	0.036	0.258
+-2.5	0.144	0.125	0.098	0.019	0.303	0.081	0.087	0.143
+-1.5	0.001	0.264	0.132	0.042	0.06	0.069	0.41	0.021
+-0.5	0.029	0.268	0.025	0.028	0.006	0.373	0.078	0.193

Table S22: $m_J(z)$ composition of the lowest 8 Kramers Doublets for compound **1**using the bare molecule, the MeOH molecule H bonded to it as well a the closest counter ion as the model compound. Orbitals are optimized with ROHF.

$m_J(z)$	KD1	KD2	KD3	KD4	KD5	KD6	KD7	KD8
+-7.5	0.241	0.014	0.045	0.108	0.358	0.114	0.062	0.059
+-6.5	0.01	0.038	0.123	0.58	0.081	0.002	0.11	0.056
+-5.5	0.443	0.031	0.006	0.075	0.005	0.047	0.234	0.16
+-4.5	0.067	0.199	0.221	0.086	0.116	0.105	0.194	0.012
+-3.5	0.152	0.029	0.167	0.076	0.377	0.062	0.049	0.087
+-2.5	0.018	0.32	0.048	0.003	0.035	0.362	0.169	0.045
+-1.5	0.024	0.19	0.24	0.051	0.002	0.094	0.072	0.327
+-0.5	0.046	0.179	0.15	0.021	0.026	0.215	0.11	0.254

Table S23: $m_J(z)$ composition of the lowest 8 Kramers Doublets for compound **1**using the bare molecule, the MeOH molecule H bonded to it as well a the two closest counter ions as the model compound. Orbitals are optimized with ROHF.

$m_J(z)$	KD1	KD2	KD3	KD4	KD5	KD6	KD7	KD8
+-7.5	0.29	0.009	0.101	0.242	0.248	0.078	0.016	0.016
+-6.5	0.015	0.029	0.065	0.188	0.134	0.032	0.397	0.14
+-5.5	0.159	0.003	0.034	0.336	0.168	0.006	0.243	0.049
+-4.5	0.428	0.115	0.036	0.009	0.22	0.1	0.089	0.004
+-3.5	0.053	0.401	0.265	0.114	0.057	0.021	0.03	0.06
+-2.5	0.006	0.298	0.154	0.071	0.107	0.344	0.013	0.006
+-1.5	0.037	0.053	0.254	0.04	0.058	0.192	0.111	0.256
+-0.5	0.013	0.092	0.091	0	0.007	0.227	0.1	0.469

Table S24: $m_J(z)$ composition of the lowest 8 Kramers Doublets for compound **1**using the bare molecule, the MeOH molecule H bonded to it as well a the three closest counter ions as the model compound. Orbitals are optimized with ROHF.

$m_J(z)$	KD1	KD2	KD3	KD4	KD5	KD6	KD7	KD8
+-7.5	0.307	0.009	0.118	0.267	0.217	0.065	0.008	0.009
+-6.5	0.019	0.028	0.045	0.09	0.131	0.039	0.498	0.15
+-5.5	0.081	0.002	0.047	0.361	0.272	0.004	0.206	0.026
+-4.5	0.51	0.069	0.02	0.047	0.188	0.096	0.064	0.007
+-3.5	0.031	0.564	0.207	0.078	0.011	0.03	0.022	0.057
+-2.5	0.007	0.222	0.288	0.129	0.091	0.243	0.003	0.016
+-1.5	0.039	0.034	0.197	0.026	0.087	0.341	0.093	0.184
+-0.5	0.007	0.072	0.078	0.003	0.003	0.182	0.106	0.55

Table S25: $m_J(z)$ composition of the lowest 8 Kramers Doublets for compound **1**using the bare molecule as the model compound. Orbitals are optimized with ROHF and CASSCF.

$m_J(z)$	KD1	KD2	KD3	KD4	KD5	KD6	KD7	KD8
+-7.5	0.282	0.019	0.003	0.066	0.36	0.137	0.027	0.106
+-6.5	0.118	0.022	0.019	0.406	0.019	0.214	0.062	0.138
+-5.5	0.036	0.029	0.276	0.327	0.065	0.026	0.166	0.075
+-4.5	0.326	0.057	0.072	0.06	0.123	0.028	0.266	0.067
+-3.5	0.032	0.243	0.353	0.029	0.015	0.042	0.06	0.226
+-2.5	0.175	0.124	0.088	0.019	0.313	0.061	0.06	0.159
+-1.5	0.022	0.242	0.142	0.052	0.079	0.076	0.315	0.071
+-0.5	0.009	0.264	0.046	0.041	0.026	0.415	0.043	0.156

Table S26: $m_J(z)$ composition of the lowest 8 Kramers Doublets for compound **1**using the bare molecule and the MeOH molecule hydrogen bonded to it as the model compound. Orbitals are optimized with ROHF and CASSCF.

$m_J(z)$	KD1	KD2	KD3	KD4	KD5	KD6	KD7	KD8
+-7.5	0.312	0.013	0.001	0.036	0.403	0.095	0.034	0.106
+-6.5	0.091	0.043	0.022	0.522	0.012	0.191	0.009	0.11
+-5.5	0.09	0.012	0.289	0.302	0.036	0.087	0.058	0.126
+-4.5	0.311	0.084	0.035	0.029	0.147	0.066	0.281	0.047
+-3.5	0.018	0.202	0.375	0.014	0.05	0.033	0.031	0.276
+-2.5	0.148	0.09	0.118	0.021	0.3	0.08	0.123	0.121
+-1.5	0.001	0.267	0.13	0.044	0.043	0.111	0.393	0.01
+-0.5	0.029	0.289	0.03	0.031	0.008	0.338	0.071	0.203

Table S27: $m_J(z)$ composition of the lowest 8 Kramers Doublets for compound **1**using the bare molecule, the MeOH molecule H bonded to it as well a the closest counter ion as the model compound. Orbitals are optimized with ROHF and CASSCF.

$m_J(z)$	KD1	KD2	KD3	KD4	KD5	KD6	KD7	KD8
+-7.5	0.25	0.013	0.061	0.111	0.351	0.105	0.063	0.046
+-6.5	0.01	0.038	0.156	0.502	0.092	0.004	0.142	0.056
+-5.5	0.42	0.025	0.01	0.1	0.009	0.043	0.267	0.126
+-4.5	0.097	0.2	0.185	0.087	0.14	0.1	0.181	0.01
+-3.5	0.144	0.042	0.18	0.107	0.339	0.059	0.057	0.072
+-2.5	0.014	0.341	0.025	0.001	0.044	0.392	0.138	0.045
+-1.5	0.024	0.172	0.241	0.073	0.003	0.068	0.063	0.357
+-0.5	0.041	0.169	0.143	0.019	0.022	0.229	0.089	0.288

Table S28: $m_J(z)$ composition of the lowest 8 Kramers Doublets for compound **1**using the bare molecule, the MeOH molecule H bonded to it as well a the two closest counter ions as the model compound. Orbitals are optimized with ROHF and CASSCF.

$m_J(z)$	KD1	KD2	KD3	KD4	KD5	KD6	KD7	KD8
+-7.5	0.305	0.007	0.129	0.224	0.241	0.069	0.014	0.011
+-6.5	0.015	0.03	0.074	0.144	0.138	0.035	0.449	0.116
+-5.5	0.135	0.002	0.051	0.338	0.191	0.006	0.245	0.032
+-4.5	0.452	0.099	0.033	0.013	0.224	0.094	0.08	0.005
+-3.5	0.043	0.451	0.224	0.131	0.042	0.019	0.033	0.056
+-2.5	0.005	0.276	0.175	0.103	0.099	0.326	0.009	0.006
+-1.5	0.036	0.046	0.229	0.045	0.06	0.241	0.093	0.25
+-0.5	0.01	0.088	0.085	0.002	0.004	0.21	0.077	0.523

Table S29: $m_J(z)$ composition of the lowest 8 Kramers Doublets for compound **1**using the bare molecule as the model compound. Orbitals are optimized with ROHF. No hydrogen positions were optimized.

$m_J(z)$	KD1	KD2	KD3	KD4	KD5	KD6	KD7	KD8
+-7.5	0.26	0.027	0.004	0.048	0.373	0.145	0.03	0.114
+-6.5	0.115	0.016	0.004	0.466	0.004	0.207	0.057	0.132
+-5.5	0.047	0.028	0.305	0.292	0.063	0.019	0.156	0.09
+-4.5	0.331	0.064	0.069	0.045	0.115	0.023	0.296	0.058
+-3.5	0.017	0.276	0.319	0.035	0.017	0.045	0.05	0.241
+-2.5	0.202	0.086	0.09	0.015	0.339	0.051	0.058	0.159
+-1.5	0.019	0.245	0.146	0.053	0.065	0.098	0.322	0.052
+-0.5	0.01	0.258	0.062	0.047	0.024	0.412	0.032	0.155

Table S30: $m_J(z)$ composition of the lowest 8 Kramers Doublets for compound **1**using the bare molecule and the MeOH molecule hydrogen bonded to it as the model compound. Orbitals are optimized with ROHF. No hydrogen positions were optimized.

$m_J(z)$	KD1	KD2	KD3	KD4	KD5	KD6	KD7	KD8
+-7.5	0.303	0.014	0.002	0.047	0.398	0.098	0.031	0.107
+-6.5	0.099	0.031	0.012	0.479	0.01	0.212	0.022	0.134
+-5.5	0.056	0.015	0.307	0.305	0.053	0.059	0.102	0.102
+-4.5	0.327	0.075	0.048	0.041	0.137	0.045	0.276	0.051
+-3.5	0.029	0.225	0.363	0.028	0.024	0.036	0.044	0.25
+-2.5	0.162	0.11	0.097	0.019	0.31	0.08	0.073	0.149
+-1.5	0.005	0.257	0.136	0.047	0.06	0.081	0.384	0.028
+-0.5	0.018	0.272	0.034	0.034	0.009	0.387	0.067	0.178

Table S31: $m_J(z)$ composition of the lowest 8 Kramers Doublets for compound **1**using the bare molecule, the MeOH molecule H bonded to it as well a the closest counter ion as the model compound. Orbitals are optimized with ROHF. No hydrogen positions were optimized.

$m_J(z)$	KD1	KD2	KD3	KD4	KD5	KD6	KD7	KD8
+-7.5	0.243	0.011	0.011	0.018	0.423	0.123	0.064	0.108
+-6.5	0.026	0.04	0.076	0.804	0.02	0.024	0.011	0.001
+-5.5	0.449	0.032	0.082	0.021	0.003	0.103	0.065	0.244
+-4.5	0.046	0.145	0.311	0.05	0.015	0.105	0.293	0.035
+-3.5	0.122	0.108	0.008	0.004	0.445	0.067	0.023	0.222
+-2.5	0.06	0.103	0.257	0.033	0.055	0.115	0.327	0.05
+-1.5	0.015	0.28	0.117	0.005	0.015	0.354	0.091	0.123
+-0.5	0.039	0.282	0.139	0.065	0.025	0.108	0.126	0.217

$m_J(z)$ composition of the lowest 8 Kramers Doublets for compound **1**using the bare molecule, the MeOH molecule H bonded to it as well a the two closest counter ions as the model compound. Orbitals are optimized with ROHF. No hydrogen positions were optimized.

$m_J(z)$	KD1	KD2	KD3	KD4	KD5	KD6	KD7	KD8
+-7.5	0.244	0.007	0.022	0.133	0.358	0.118	0.048	0.069
+-6.5	0.002	0.029	0.058	0.64	0.092	0.002	0.104	0.074
+-5.5	0.449	0.014	0.002	0.085	0.01	0.048	0.189	0.202
+-4.5	0.077	0.222	0.246	0.031	0.103	0.105	0.208	0.009
+-3.5	0.176	0.031	0.21	0.029	0.364	0.041	0.026	0.123
+-2.5	0.009	0.358	0.032	0.005	0.031	0.343	0.19	0.032
+-1.5	0.013	0.174	0.293	0.035	0.003	0.083	0.108	0.291
+-0.5	0.03	0.166	0.137	0.044	0.039	0.259	0.126	0.199

Table S32: $m_J(z)$ composition of the lowest 8 Kramers Doublets for compound **1**using the bare molecule, the MeOH molecule H bonded to it as well a the three closest counter ions as the model compound. Orbitals are optimized with ROHF. No hydrogen positions were optimized.

$m_J(z)$	KD1	KD2	KD3	KD4	KD5	KD6	KD7	KD8
+-7.5	0.253	0.008	0.032	0.182	0.327	0.108	0.039	0.051
+-6.5	0.007	0.026	0.057	0.5	0.116	0.009	0.173	0.112
+-5.5	0.365	0.007	0.014	0.167	0.041	0.028	0.22	0.158
+-4.5	0.18	0.208	0.163	0.014	0.157	0.104	0.17	0.006
+-3.5	0.148	0.105	0.289	0.043	0.254	0.031	0.026	0.103
+-2.5	0.005	0.396	0.001	0.005	0.062	0.385	0.122	0.025
+-1.5	0.016	0.12	0.33	0.058	0.007	0.021	0.135	0.312
+-0.5	0.026	0.13	0.114	0.031	0.037	0.316	0.114	0.232

Table S33: Angles between the Er-O bond and the ground state magnetic main axis in ° for all calculated models. "opt" refers to models with H-optimization but no intermediate CASSCF calculation, "CAS" refers to models with both H-optimization and intermediate CASSCF calculation. "unopt" refers to models taken directly from the cif-file and without intermediate CASSCF calculation.

$m_J(z)$	opt	CAS	unopt
bare	86.377	86.625	89.427
MeOH	89.344	89.417	88.822
otf1	88.456	88.478	88.558
otf2	88.915	88.884	88.995
otf3	87.856	-	89.724

Table S34: Direction of g_z-axis for selected models of the first and second KD. "opt" refers to calculations with optimized hydrogen atoms and without an intermediate CASSCF calculation.

model	KD1			KD2		
	g_{zx}	g_{zy}	g_{zz}	g_{zx}	g_{zy}	g_{zz}
unopt_bare	0.51047471	0.51286667	0.69020529	-0.32135355	0.70958220	-0.62707655
unopt_full	0.57334240	0.12638724	0.80950896	-0.29044453	0.72230266	-0.62763114
opt_bare	0.56378251	0.52672880	0.63616512	-0.24900592	0.73473554	-0.63099900
opt_full	0.59453585	-0.02462431	0.80369196	0.32787571	-0.64726544	0.68814603

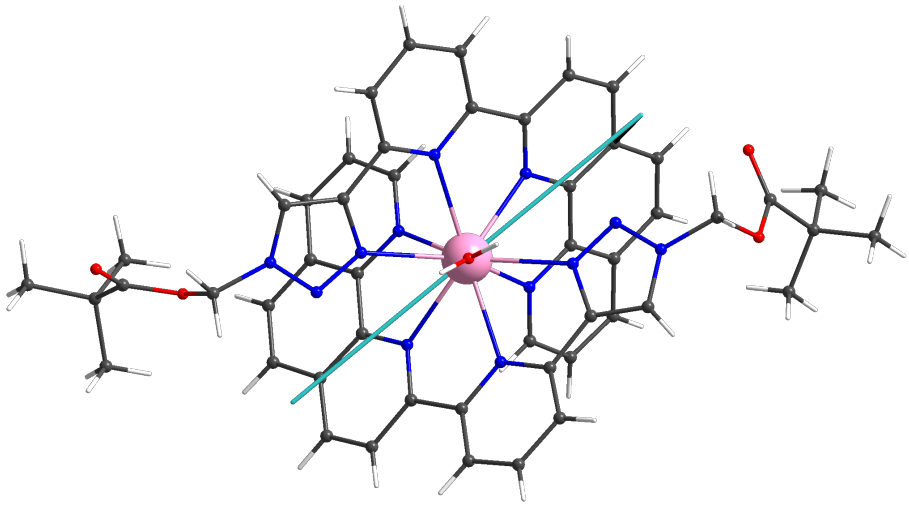

Figure S13: Calculated magnetic main axis of the ground state for the bare model with unoptimized hydrogen positions. The axis roughly follows the direction of the hydrogen positions of the water ligand.

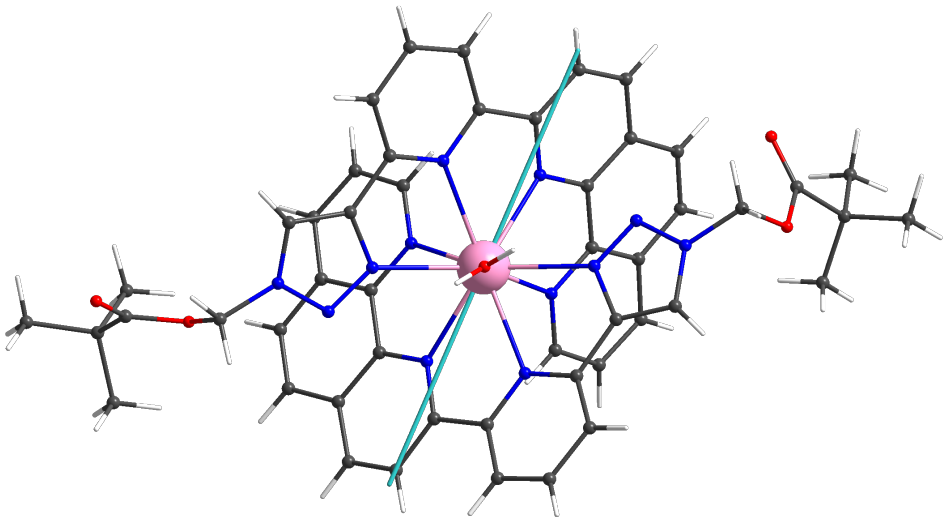

Figure S14: Calculated magnetic main axis of the ground state for the model including all counterions with unoptimized hydrogen positions. The additional MeOH and counterions are included in the calculation but omitted in this picture for simplicity.

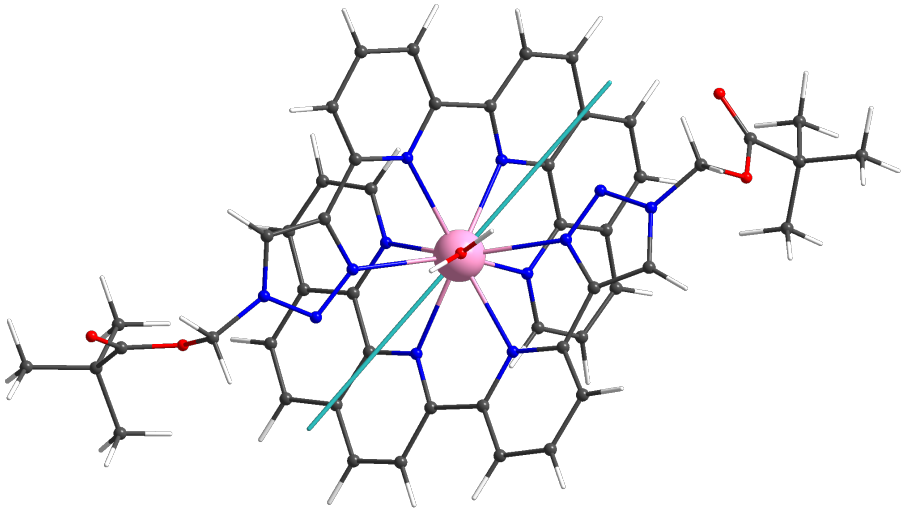

Figure S15: Calculated magnetic main axis of the ground state for the bare model with optimized hydrogen positions and no intermediate CASSCF calculation. The axis roughly follows the direction of the hydrogen positions of the water ligand.

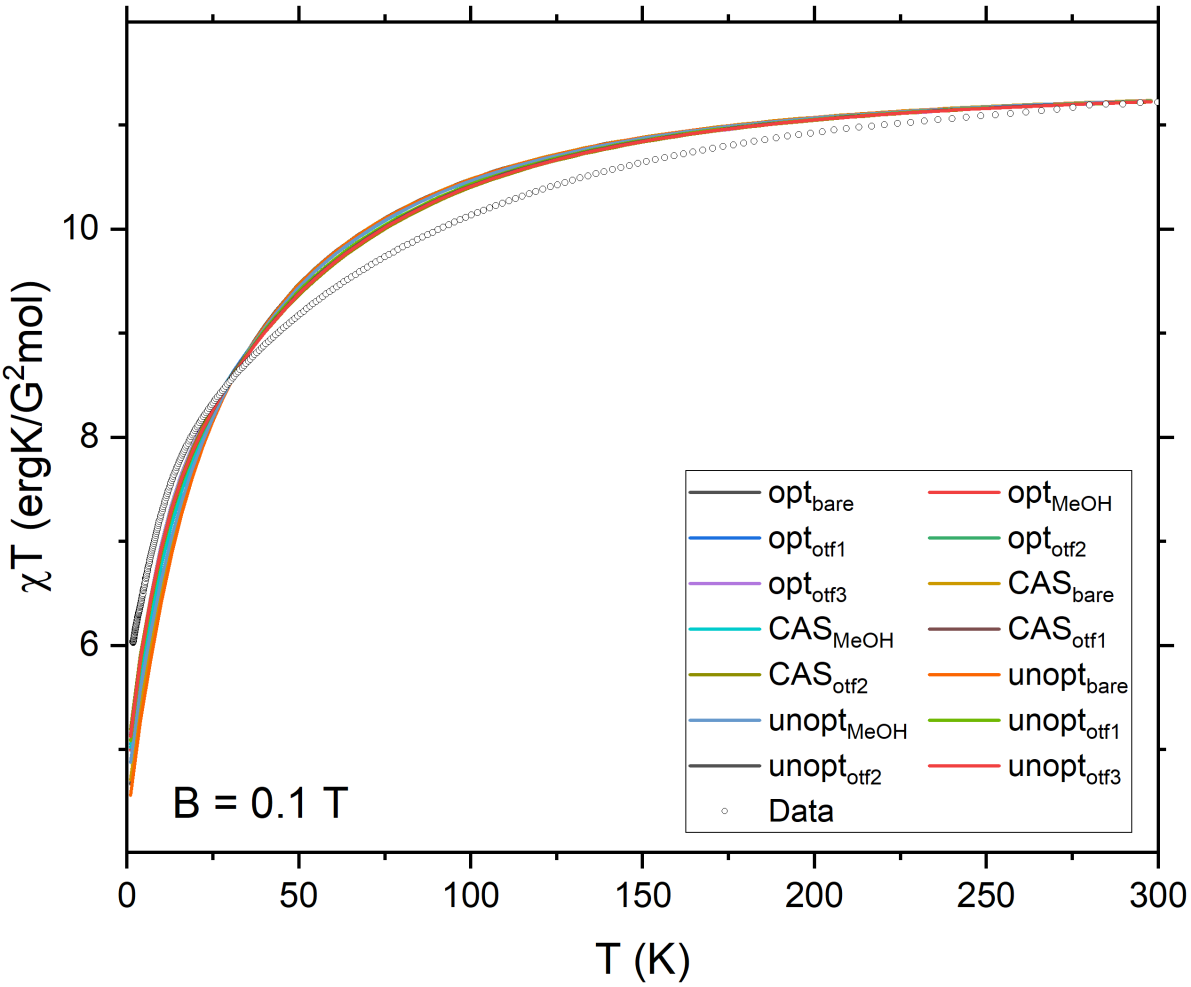

Figure S16: Calculated and measured χT-curves for all computational models. No significant deviation can be reported. "opt" refers to calculations with optimized hydrogen atoms and without an intermediate CASSCF calculation.

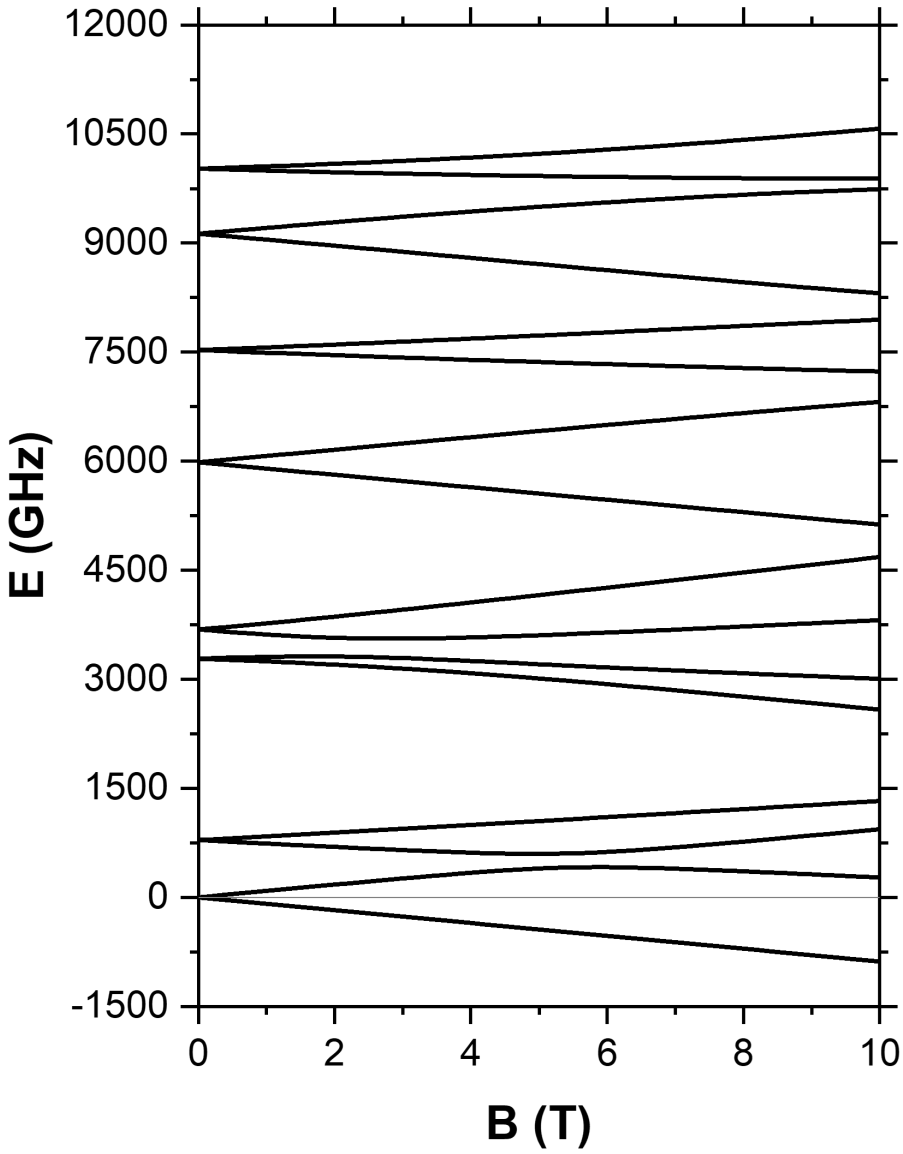

Figure S17: Zeeman diagram of all 16 states of the $^4I_{15/2}$-ground state with a magnetic field along the magnetic main axis simulating the loose powder experiment. The model is that including all counterions, optimized hydrogens and no intermediate CASSCF step.

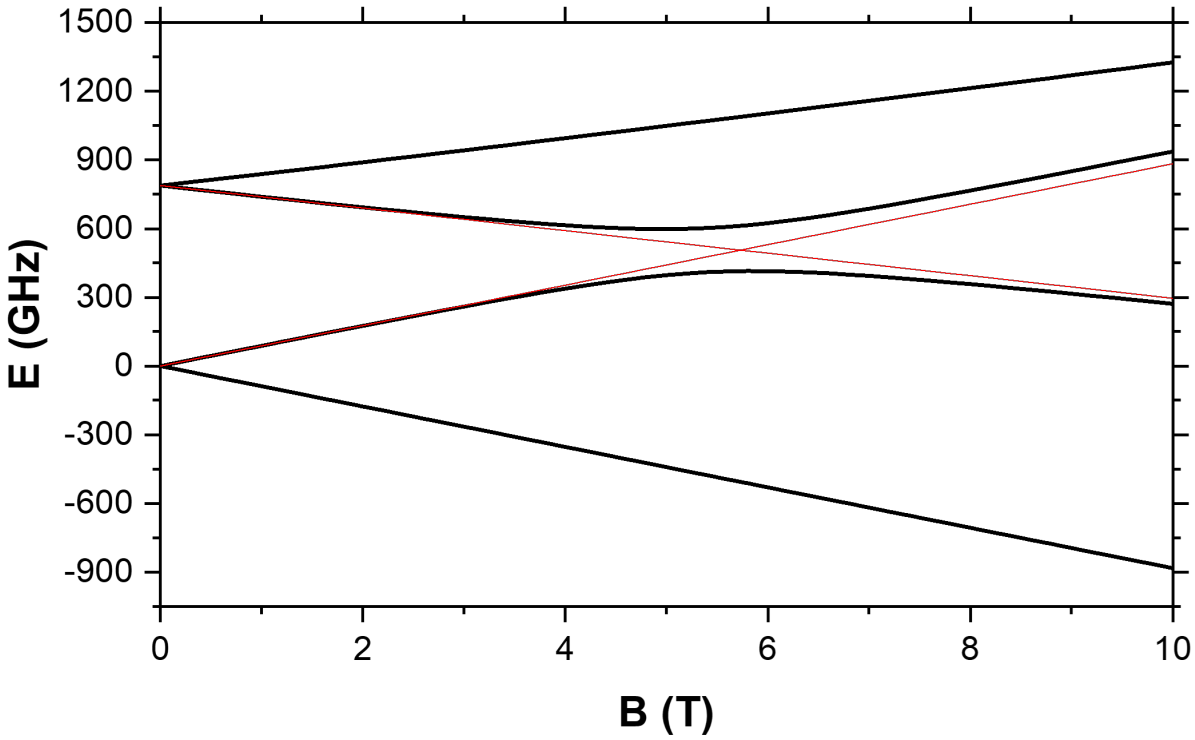

Figure S18: Zeeman diagram of the lowest four states with a magnetic field along the magnetic main axis simulating the loose powder experiment are shown in black. The red lines indicate a perfect linear behaviour, showing that a theoretical level crossing would occur at around 5.8 T. The model is that including all counterions, optimized hydrogens and no intermediate CASSCF step.

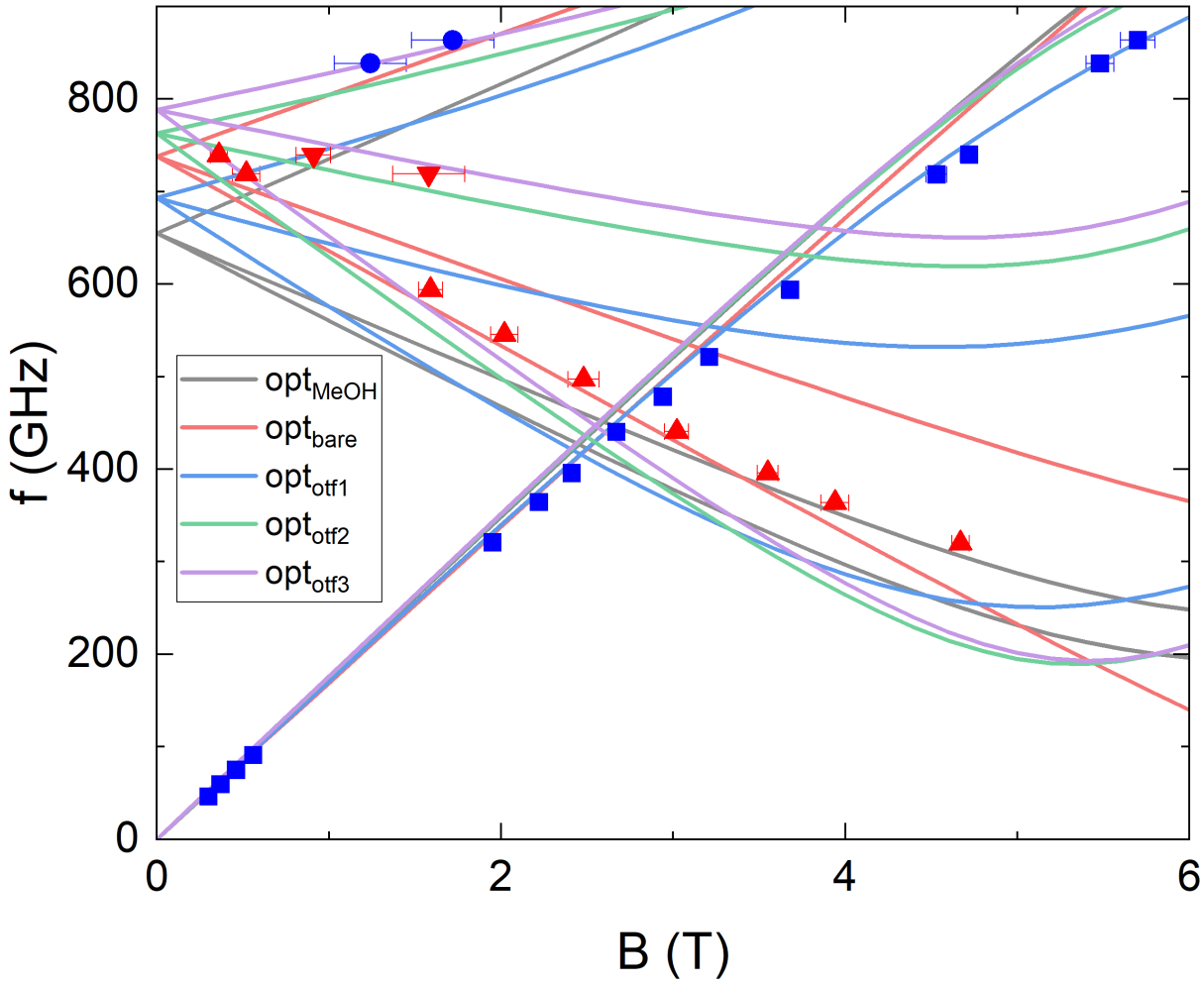

Figure S19: Measured transition energies on a loose powder (points) and calculated transition energies within the lowest two Kramers Doublets (lines) for the optimised models without an intermediate CASSCF calculation. Blue data points are measured at 2K, red data points at temperatures greater than 2K.

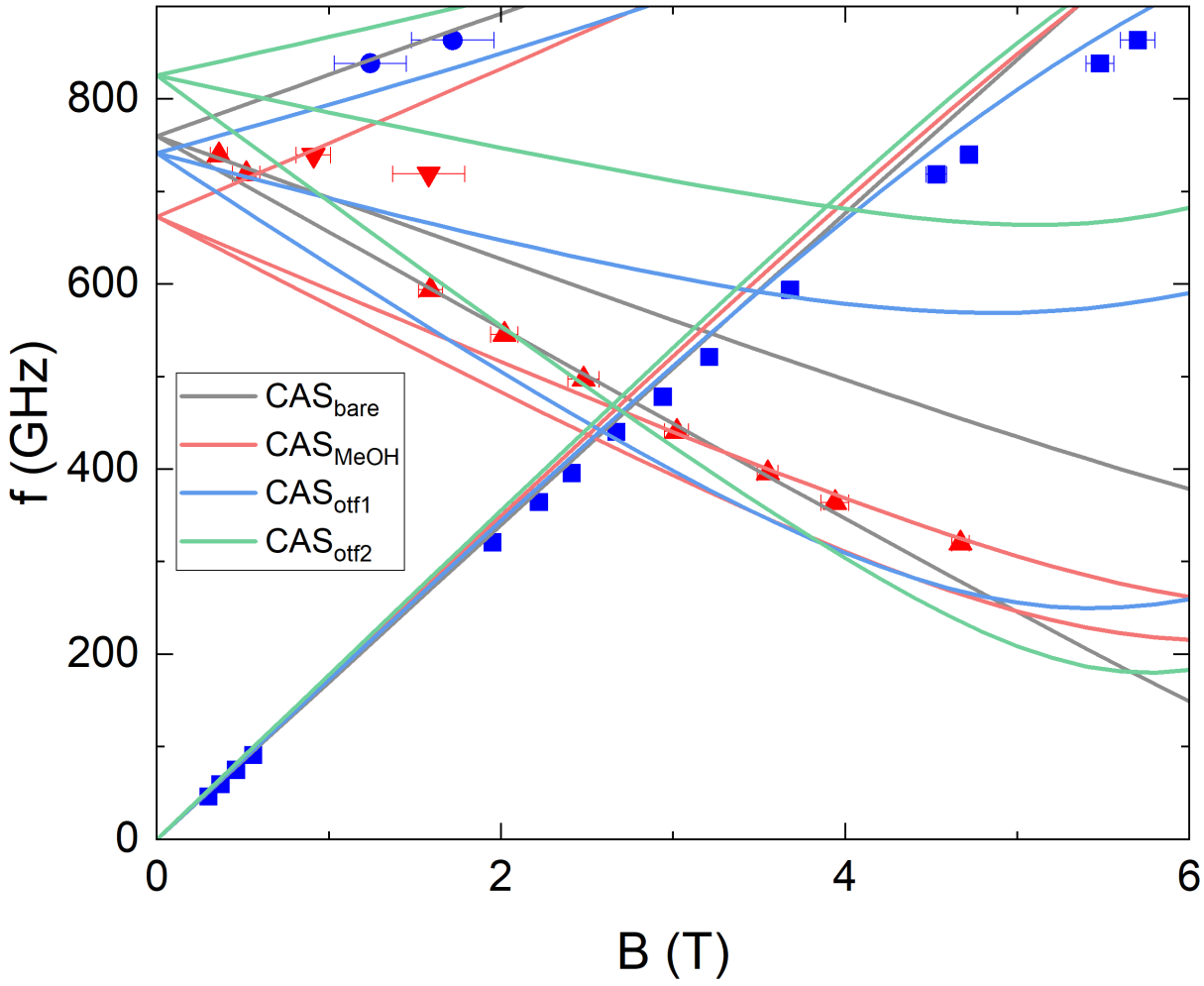

Figure S20: Measured transition energies on a loose powder (points) and calculated transition energies within the lowest two Kramers Doublets (lines) for the optimised models with an intermediate CASSCF calculation. Blue data points are measured at 2K, red data points at temperatures greater than 2K.

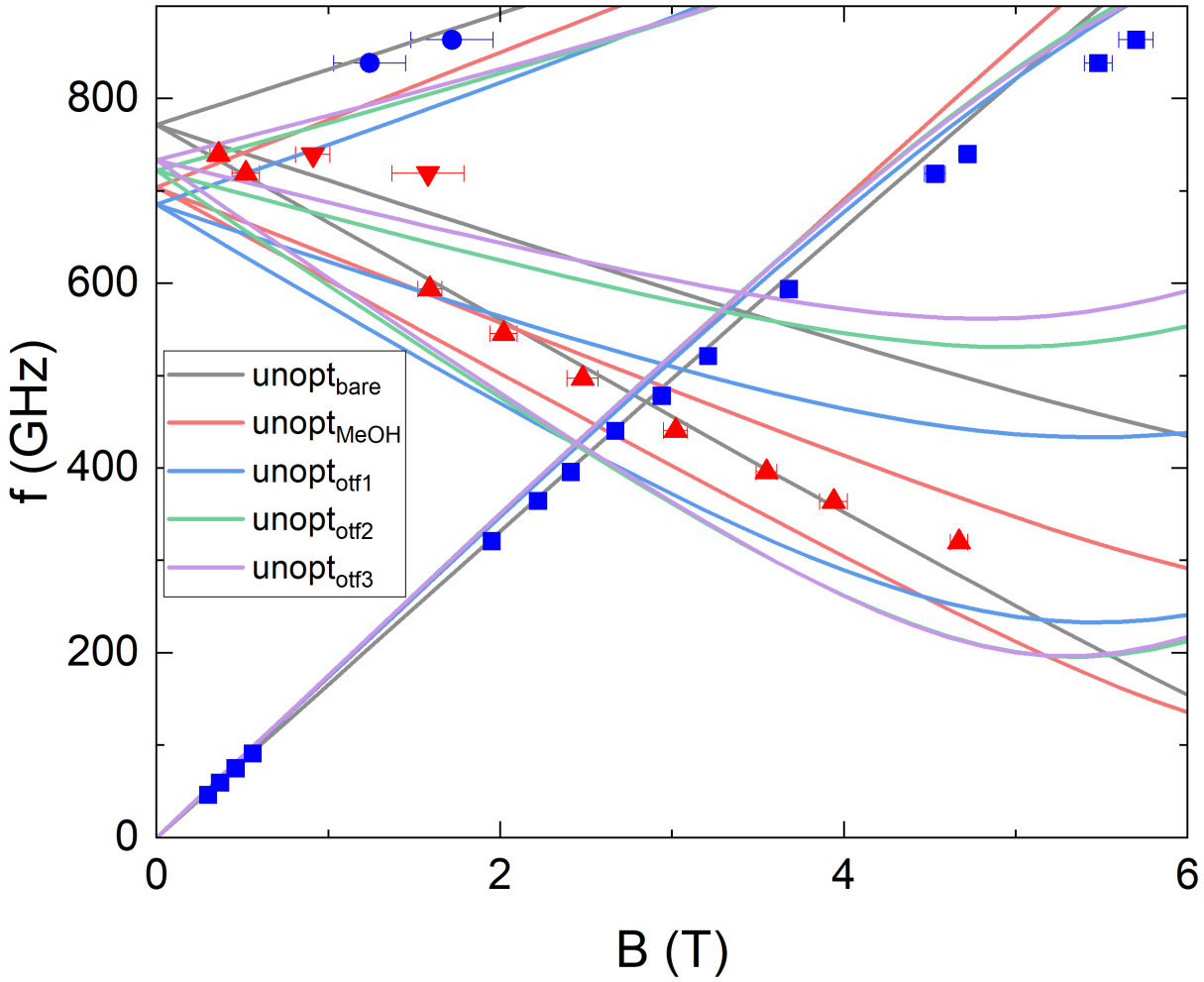

Figure S21: Measured transition energies on a loose powder (points) and calculated transition energies within the lowest two Kramers Doublets (lines) for the unoptimised models. Blue data points are measured at 2K, red data points at temperatures greater than 2K.

Table S35: R^2, Mean Absolute Errors (MAE), and Root Mean Square Deviation (RMSD) for models with optimized hydrogen positions and no intermediate CASSCF calculation. MAE and RMSD are given in GHz.

	bare	MeOH	otf1	otf2	otf3
R^2	0.979	0.917	0.966	0.968	0.977
MAE	27.587	61.848	43.090	38.682	32.546
RMSD	36.800	75.980	56.956	46.721	41.727

Table S36: R^2, Mean Absolute Errors (MAE), and Root Mean Square Deviation (RMSD) for models with optimized hydrogen positions and intermediate CASSCF calculation. MAE and RMSD are given in GHz.

	bare	MeOH	otf1	otf2
R^2	0.985	0.932	0.983	0.986
MAE	22.933	55.101	30.225	38.647
RMSD	33.734	67.098	33.719	46.121

Table S37: R^2, Mean Absolute Errors (MAE), and Root Mean Square Deviation (RMSD) for models with unoptimized hydrogen positions. MAE and RMSD are given in GHz.

	bare	MeOH	otf1	otf2	otf3
R^2	0.993	0.948	0.949	0.953	0.959
MAE	15.433	48.651	51.553	50.104	46.559
RMSD	23.359	58.416	61.411	57.167	53.535

Table S38: Different indicators of the relaxation speed as calculated for the 5 different models. "opt" refers to the models with optimized H-positions and no intermediate CASSCF calculation. "CAS" refers to models with intermediate CASSCF calculation and optimized H-positions. "unopt" refers to models directly taken from the .cif-file. The relaxation time is calculated in two ways: The model suggested by Yin *et al.* based on time dependent perturbation theory[5,6] and the by Prokof'ev and Stamp based on instanton theory.[7–9] All relaxation times are give in $10^{-8}\,s$. Lastly, we report the magnetic transition moment between the two states in the lowest KD.

	opt			CAS			unopt		
model	Yin	PS	TM	Yin	PS	TM	Yin	PS	TM
bare	2.2	0.4	0.2998	2.5	0.5	0.2770	1.3	0.3	0.4171
MeOH	1.5	0.3	0.3813	1.5	0.3	0.3971	5.5	1.1	0.1646
otf1	0.5	0.0	0.7228	0.5	0.1	0.6695	0.7	0.1	0.5801
otf2	0.9	0.2	0.5154	1.2	0.2	0.4493	0.9	0.2	0.5132
otf3	0.9	0.2	0.5091	-	-	-	0.9	0.2	0.5187

The formula used to calculate the tunnelling times using the model published by Yin *et al.*.[5,6]

$$\tau_{QTM} = \frac{h}{\mu_B \cdot B} \cdot \frac{\sqrt{g_x^2 + g_y^2 + g_z^2}}{g_x^2 + g_y^2} \tag{1}$$

The formula used to calculate the tunnelling times using the model published by Prokof'ev and Stamp.[7–9]

$$\tau_{QTM} = \frac{h}{\mu_B \cdot B} \cdot \frac{g_z}{2 \cdot \sqrt{2\pi} \cdot (g_x^2 + g_y^2)} \tag{2}$$

Both equations depend on an internal (here isotropic) B-field which is assumed as 0.02 T according to the original publications. The tunneling time and relaxation rate ω can be calculated as

$$\tau_{QTM} = \frac{1}{2\omega_{QTM}} \tag{3}$$

References

(1) Zong, R.; Wang, D.; Hammitt, R.; Thummel, R. P. Synthetic Approaches to Polypyridyl Bridging Ligands with Proximal Multidentate Binding Sites. *J. Org. Chem.* **2005**, *71*, 167–175.

(2) Peng, D.; Middendorf, N.; Weigend, F.; Reiher, M. An Efficient Implementation of Two-Component Relativistic Exact-Decoupling Methods for Large Molecules. *J. Chem. Phys.* **2013**, *138*, 184105.

(3) van Wüllen, C. Relation between Different Variants of the Generalized Douglas-Kroll Transformation through Sixth Order. *J. Chem. Phys.* **2004**, *120*, 7307–13.

(4) van Wüllen, C.; Michauk, C. Accurate and Efficient Treatment of Two-Electron Contributions in Quasirelativistic High-Order Douglas-Kroll Density-Functional Calculations. *J. Chem. Phys.* **2005**, *123*, 204113.

(5) Yin, B.; Li, C.-C. A Method to Predict Both the Relaxation Time of Quantum Tunneling of Magnetization and the Effective Barrier of Magnetic Reversal for a Kramers Single-Ion Magnet. *Phys. Chem. Chem. Phys.* **2020**, *22*, 9923–9933.

(6) Yin, B.; Luo, L. The Anisotropy of the Internal Magnetic Field on the Central Ion Is Capable of Imposing Great Impact on the Quantum Tunneling of Magnetization of Kramers Single-Ion Magnets. *Phys. Chem. Chem. Phys.* **2021**, *23*, 3093–3105.

(7) Prokof'ev, N. V.; Stamp, P. C. E. Quantum Relaxation of Magnetisation in Magnetic Particles. *J. Low Temp. Phys.* **1996**, *104*, 143–209.

(8) Prokof'ev, N. V.; Stamp, P. C. E. Theory of the Spin Bath. *Rep. Prog. Phys.* **2000**, *63*, 669–726.

(9) Luis, F.; Martínez-Pérez, M. J.; Montero, O.; Coronado, E.; Cardona-Serra, S.; Martí-Gastaldo, C.; Clemente-Juan, J. M.; Sesé, J.; Drung, D.; Schurig, T. Spin-Lattice Relaxation via Quantum Tunneling in an Er^{3+}-Polyoxometalate Molecular Magnet. *Phys. Rev. B* **2010**, *82*, 060403.